Gas Chromatographic Method Development for Analysis of Samples from a Carbon Capture Pilot Plant

by

David Wedin

Department of Chemical Engineering
Lund University

June 2023

Supervisor: **Helena Svensson, Lund University**
Co-supervisor: **Hanna Karlsson, Lund University**
Examiner: **Ola Wallberg, Lund University**

Picture on front page: Photo by David Wedin

Postal address	**Visiting address**	**Telephone**
P.O. Box 124	Getingevägen 60	+46 46-222 82 85
SE-221 00 Lund, Sweden		+46 46-222 00 00
Web address		
www.chemeng.lth.se		

Acknowledgments

This page is dedicated to all the people who have helped and supported me throughout this Master's Thesis. I would like to start by expressing my gratitude to my supervisor, Helena Svensson and my co-supervisor, Hanna Karlsson, for the opportunity to be part of this project. Your expertise and constructive feedback have played a pivotal role in sharpening the direction and quality of this thesis. You have also been helpful and supportive throughout the research process, for which I am very thankful.

I would also like to thank the people at the Department of Chemical Engineering, especially the people on floor +1. I appreciate that you never hesitate to offer your valuable help and insights. Thank you, Ola Wallberg, for being my examiner. Also, a special thanks to Selda Bekirovska and Mats Galbe for your tremendous help with battling the GC with me. Thanks to Isac Logeke as well. Sharing the office with you have been very valuable for this thesis, but also for me personally. Best of luck in the future.

I would also like to thank my friends and family for your support throughout my time at LTH. It would have been substantially more difficult without you.

Lastly, I would like to include a quote said by my first chemistry teacher, said on my very first chemistry lecture, which is the reason why I got interested in chemistry in the first place:

''Everything is chemistry''

Abstract

In response to the escalating threat of climate change, carbon capture and storage have gained increasing attention as an important component in mitigating the global carbon dioxide emissions. Substantial research efforts have focused on enhancing the energy efficiency and availability of these technologies. At the Department of Chemical Engineering at Lund University, research is being carried out to investigate a novel absorption system and its potential as an alternative to more conventional systems. The absorption mixture consists of the sterically hindered amine 2-amino-2-metyl-1-propanol (AMP) and the organic solvent dimethyl sulfoxide (DMSO). As part of the research, the absorption system is being tested and evaluated on a pilot plant scale, operating in an industrial setting at Växjö Energi AB. In this thesis, gas chromatographic methods were investigated as analysis methods for measuring AMP and DMSO concentrations in the pilot plant. Both qualitative and quantitative analysis were performed, and the methods were validated based on selectivity, linearity and precision. Three different solvents were investigated, acetonitrile, sulfamic acid and sulfuric acid.

The results showed that qualitative and quantitative gas chromatographic analysis can be performed to give estimations of the AMP and DMSO concentrations. Acetonitrile proved to perform best as the solvent and a linear response between detector response and concentration could be obtained for both AMP and DMSO. The results also suggested that large amounts of water in samples analyzed with the gas chromatographic set up caused unstable detector response.

Analysis of samples from the pilot plant demonstrated a more pronounced concentration decrease of AMP compared to DMSO, after gas streams were introduced into the pilot, indicating that AMP likely participates in reactions. It was also shown that the concentrations of AMP and DMSO in the gas streams leaving the pilot were small, implying that the implementation of this absorption system into various processes would result in only minor emissions of the absorption mixture.

Populärvetenskaplig sammanfattning

Som svar på det eskalerande hotet från klimatförändringar har koldioxidinfångning fått alltmer uppmärksamhet som en viktig teknik för att minska de globala koldioxidutsläppen. Stora forskningsinsatser fokuserar nu på att förbättra energieffektiviteten och tillgängligheten för dessa tekniker. Vid Institutionen för Kemiteknik vid Lunds Universitet, bedrivs forskning för att undersöka ett nytt absorptionssystem för koldioxidinfångning och dess potential som ett alternativ till mer traditionella system. Absorptionssystemet består av den steriskt hindrade aminen 2-amino-2-metyl-1-propanol (AMP) och det organiska lösningsmedlet dimetylsulfoxid (DMSO). Som en del i forskningsprojektet testas systemet i pilotskala på en industriell anläggning på Växjö Energi AB. I detta examensarbete har gaskromatografiska metoder undersökts som analysmetoder för att mäta AMP- och DMSO-koncentrationer i pilotanläggningen. Både kvalitativ och kvantitativ analys utfördes och metoderna validerades baserat på selektivitet, linjäritet och precision. Tre lösningsmedel testades, acetonitril, sulfaminsyra och svavelsyra.

Resultaten från undersökningarna visade att både kvalitativ och kvantitativ gaskromatografisk analys kunde genomföras för att ge en uppskattad koncentration av AMP och DMSO. Acetonitril visade sig fungera bäst som lösningsmedel och ett linjärt samband mellan detektorrespons och koncentration erhölls för både AMP och DMSO. Resultaten antydde också att för stora mängder vatten i proverna som analyserades i gaskromatografen orsakade instabil detektorrespons.

Analys av prover från pilotanläggningen kunde också visa på en större koncentrationsminskning av AMP jämfört med DMSO, efter att absorptionslösningen passerat absorptionstornet, vilket indikerar att AMP troligtvis deltar i reaktioner. Det kunde också visas att koncentrationerna av AMP och DMSO i gasflödena ut ur piloten var små, vilket innebär att implementeringen av detta absorptionssystem i olika processer troligtvis endast skulle resultera i mindre utsläpp av absorptionsblandningen.

Nomenclature

Abbreviations

GC	Gas chromatography
AMP	2-amino-2-methyl-1-propanol
DMSO	Dimethyl sulfoxide
MEA	Monoethanolamine
NMP	n-methyl-2-pyrrolidon
NDMA	n-nitrosodimethylamine
FID	Flame ionization detector
OPGC	Optimal practical gas velocity
CCS	Carbon capture and storage
VEAB	Växjö Energi AB

Abbreviations for samples

AA	Acetonitrile + AMP
AD	Acetonitrile + DMSO
AAD	Acetonitrile + AMP + DMSO
AADM	Acetonitrile + AMP + DMSO + MEA

Symbols

R_s	Resolution
t_R	Retention time
t'_R	Adjusted retention time
t_M	Shortest possible retention time
α_s	Separation factor
$w_{1/2}$	Peak width at half peak height
$w_{1/2av}$	Average peak width at half peak height
w_{av}	Average peak width
F	Response factor
A	GC area

H	Plate height
u_x	Linear velocity
P_{vap}	Vapor pressure
H_{vap}	Enthalpy of evaporation
R	Gas constant
T	Temperature
DF	Dilution factor
V	Volume
c	Concentration
m	Mass
R^2	Square of the correlation coefficients
s	Standard deviation

Table of Contents

1 INTRODUCTION 1
1.2 Aim 2

2 THEORY 3

2.1 Carbon Capture and Storage (CCS) 3

2.2 The pilot plant 4

2.3 Sampling methods 6

2.4 The Chromatogram 8
2.4.1 Qualitative analysis using chromatograms 9
2.4.2 Quantitative analysis using chromatograms 10

2.5 Gas Chromatography (GC) 11
2.5.1 Column 12
2.5.2 Detector 13
2.5.3 Sample injection 13
2.5.4 Carrier gas 15
2.5.5 Temperature and Pressure 16
2.5.6 Sample preparation 18

2.6 GC Trouble shooting 18
2.6.1 Ghost Peaks and Carry over 18
2.6.2 Extensive Baseline Noise 19
2.6.3 Baseline Instability or Disturbances 19
2.6.4 Fronting Peaks 19
2.6.5 Tailing peaks 20
2.6.6 Split peaks 20
2.6.7 Retention Time Shift 20
2.6.8 Change in Peak Size 21
2.6.9 Loss of Resolution 21

3 MATERIALS AND METHODS 23

3.1 Equipment and Chemicals 23

3.2 Qualitative analysis 25

3.3 Quantitative analysis 26
3.3.1 External Standard Method 26
3.3.2 Internal Standard Method 27

3.4 Analysis of Samples from Pilot Plant 28

3.5 Method validation 31
3.5.1 Selectivity 31
3.5.2 Linearity 31
3.5.3 Precision 32

4 RESULTS AND DISCUSSION 33

4.1 Qualitative analysis 33
4.1.1 Acetonitrile as solvent 33
4.1.2 Sulfamic acid as solvent 34
4.1.3 Sulfuric acid as solvent 36

4.2 Quantitative analysis 38
4.2.1 External Standard Method 38
4.2.2 Internal Standard Method 42

4.3 Analysis of Samples from Pilot Plant 44

5 CONCLUSION 49

6 FUTURE WORK 51

7 REFERENCES 53

APPENDIX A – GC METHOD SETTINGS FOR ACETONITRILE AND SULFURIC ACID 55

APPENDIX B – GC METHOD SETTINGS FOR SULFAMIC ACID 59

APPENDIX C – EXTERNAL CALIBRATION CURVES FOR PILOT PLANT SAMPLE SET 1 61

APPENDIX D – EXTERNAL CALIBRATION CURVES FOR PILOT PLANT SAMPLE SET 2 65

APPENDIX E – EXTERNAL CALIBRATION CURVES FOR PILOT PLANT SAMPLE SET 3 69

1 Introduction

In the face of a rapidly changing climate, humanity finds itself standing at a critical time. The increasing concentrations of carbon dioxide (CO_2), and other greenhouse gases, in the atmosphere over the last decades have caused the global temperature to rise at a rate not observed over many millennia.[1] The effects of climate change have given cause for major concerns and in 1997, the Kyoto Protocol[2] was adopted as an effort to mitigate its impact. This became the first legally binding international treaty that aimed to reduce the emissions of greenhouse gases, by committing the signing countries to develop programs for this cause. In 2015, the Kyoto Protocol was replaced by the Paris Agreement[3] with more ambitious goals. The Paris Agreement aims to limit greenhouse gas emissions to levels that would keep the average global temperature below 1.5°C, compared to before the industrial revolution.[3] Despite this, the CO_2 concentrations keep increasing in the atmosphere. In April 2023 the concentration of CO_2 was measured at 421 ppm, compared to 403 ppm in December 2015[4], when the Paris Agreement was adopted, and compared to pre-industrial levels of around 280 ppm[5]. To stop this trend and to meet the Paris Agreement, a lot of focus has been put on phasing out fossil fuels and replacing them with renewable energy sources. The urgency to reduce the CO_2-levels has however caused CO_2-reducing technologies, including carbon capture and storage (CCS), to attract notice. The Swedish government has commissioned the Swedish Energy Agency to promote CCS in Sweden to reach the goal of net zero emissions of greenhouse gases by 2045.[6]

CCS is a technique in which the CO_2 from industrial processes and power plants is separated from the flue gas and captured, instead of being emitted into the atmosphere. The CO_2 can then be permanently stored, by for example injecting it deep into the subsurface of the earth, with the goal of it eventually turning into stone.[7] By combining this technique with using biofuels for the combustion, negative emissions could even be achieved.[8] Biofuels are generally considered carbon-neutral since the same amount of CO_2 is emitted during combustion, as initially absorbed during the growth of the crops. By capturing the carbon from combustion of biofuels, atmospheric CO_2 concentrations can hence be reduced. One of the primary challenges associated with CCS processes is their high cost and energy demand. Compared to simply emitting the CO_2-rich flue gas, additional money and energy must be invested to capture, compress and transfer the CO_2. Making CCS less energy-demanding and thus more economically feasible is hence essential to make it a valid option to implement in industries.[7-9]

At the Department of Chemical Engineering at Lund University, research is carried out to investigate a novel CO_2 absorption system and its potential as an alternative to more conventional CCS systems. The absorption technique, developed at the university, utilizes the sterically hindered amine 2-amino-2-metyl-1-propanol (AMP) in the organic solvent dimethyl sulfoxide (DMSO).[9] AMP is a common amine for CO_2 absorption, but it is usually used in an aqueous solution. The high energy demand for CCS processes is largely connected to the regeneration of the aqueous solution. The benefit of using the combination of AMP and DMSO, compared to conventional aqueous amine solutions, is that it can be generated at lower temperatures. AMP and DMSO can be generated between 70 and 90°C, while for example aqueous MEA (a well-studied absorption mixture) requires generation temperatures above 120°C. Using an absorption mixture of AMP and DMSO hence reduces the energy required to produce the heat needed for this otherwise energy-intensive step. Additionally, when AMP

reacts with CO_2, a carbamate is formed that precipitates, and can be separated from the rest of the solution. By only letting a slurry with high concentration of CO_2-rich precipitate go through to the regeneration step, the energy demand could potentially be reduced even further.[9]

This absorption system has provided promising results on a laboratory scale and in a project initiated by the university, funded by the Swedish Energy Department, this system is being tested and evaluated in pilot plant scale.[9] The project aims to investigate the absorption performance of CO_2 as well as the potential AMP and DMSO emissions when running the process on pilot plant scale. Since AMP and DMSO are a novel combination for CCS and have never been tested at this scale, their reactions with other chemicals in a reactive environment are relatively unexplored. The understanding of the atmospheric chemistry and kinetics of AMP is also limited at present. Studies has shown indications of AMP being able to enter atmospheric chemical reaction pathways by for example inhibiting ozone formation.[10] Amines could also potentially react in the air to form new structures that may be more harmful than the original amine itself.[11] Therefore, the project aims to regularly analyze samples taken from different parts of the pilot to investigate the chemical composition of AMP and DMSO and evaluate the performance of the plant.

1.2 Aim

This thesis has been performed at the Department of Chemical Engineering, as a part of the pilot plant project. The aim was to investigate and develop methods for qualitative and quantitative analysis of AMP and DMSO. The methods were then used to analyze samples from the pilot plant to assess its performance when operating at a power plant from Växjö Energi AB (VEAB). The technique used for the analyzes was gas chromatography (GC), in which several parameters in settings were tested. Three different solvents were studied: acetonitrile, sulfamic acid and sulfuric acid. Two quantitative analysis methods were also investigated: the external standard method and the internal standard method. The methods were validated based on selectivity, linearity and precision.

2 Theory

2.1 Carbon Capture and Storage (CCS)

Carbon capture process-techniques can be divided into three broad categories: *post-combustion*, *pre-combustion* and *oxy-fuel combustion*. Post-combustion techniques have gained the most interest recently because they can be relatively easily implemented into already existing processes.[12] There are a few chemical-methods that can be used to capture carbon, with absorption, adsorption and membranes being the main approaches.[13] In the absorption method, a liquid mixture of absorbent and solvent is used to interact with the CO_2 by chemical- or physical absorption, leaving the rest of the gas to exit into the atmosphere. The CO_2-rich mixture is then regenerated at high temperatures to desorb the CO_2. The absorption mixture can then be reused and the CO_2 can be compressed and stored.[12] In adsorption methods, a solid surface is used as the adsorber instead of a liquid mixture. In the membrane method, a membrane is used to separate CO_2. Both the adsorption and the membrane method are regarded as potential energy efficient methods. However, it is the absorption method that is the most commonly practiced in industry.[12, 13]

Aqueous amine solutions are common absorption mixtures for CCS, since they react selectively with acid gases like CO_2.[9] Figure 1 shows a typical flow sheet for an aqueous amine absorption process.

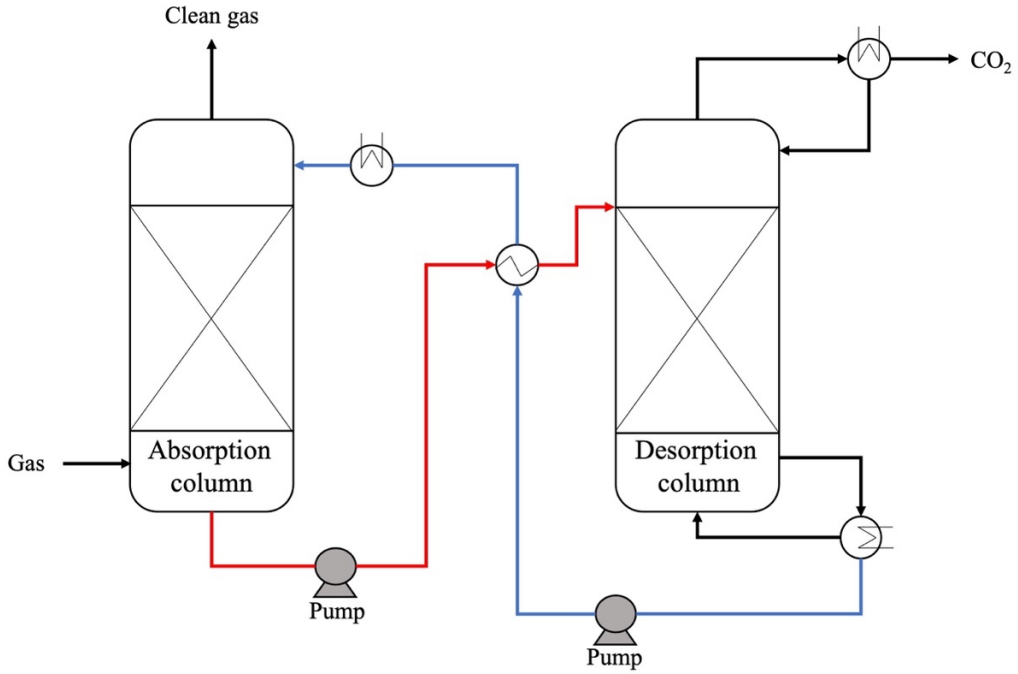

Figure 1. Schematic representation of a typical aqueous amine absorption process. The red lines indicate CO_2-rich solution and the blue lines represent lean solution.

The CO_2-containing gas from the plant enters the absorption column at the bottom. The absorption column contains the aqueous amine solution. When the gas enters, CO_2 is absorbed into the liquid, where it can react further. Which chemical-pathways that are offered depends on the amine and solvent. One possibility is that CO_2 react with the amines to form a carbamate.

The remaining gas passes through the column and exits at the top. The solution, which eventually becomes saturated with CO_2, leaves the column at the bottom. The now CO_2-rich solution enters a desorption column (or stripper column) where the temperature is raised to regenerate the solution. When the temperature is high enough, CO_2 desorbs and is collected at the top. It can then be compressed, transported and permanently stored. The lean solution is transferred back to the absorption column where it can be used to capture CO_2 again. A heat exchanger is usually used for energy recovery between the CO_2-rich and lean solution.[9]

The most well studied amine for carbon capture is monoethanolamine (MEA)[13], with the structure in Figure 2.

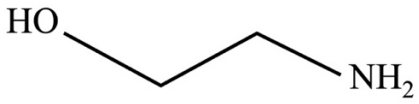

Figure 2. Chemical structure of monoethanolamine (MEA).

The reaction mechanisms for aqueous amine absorption of CO_2 can be explained with the zwitterion mechanism (Reaction 1-4).[9]

$$CO_2 + RNH_2 \leftrightarrow RNH_2^+COO^- \quad (1)$$

$$RNH_2^+COO^- + RNH_2 \leftrightarrow RNHCOO^- + RNH_3^+ \quad (2)$$

$$RNH_2^+ + H_2O \leftrightarrow HCO_3^- + RNH_3^+ \quad (3)$$

$$RNHCOO^- + H_2O \leftrightarrow HCO_3^- + RNH_2 \quad (4)$$

In Reaction 1, solved CO_2 reacts with the amine (RHN_2) to form a zwitterion intermediate. The zwitterion can then react with the amine to carbamate, see Reaction 2. Since water is present, some bicarbonate is also formed, Reaction 3 and 4. The formation of bicarbonate can be limited by using amines like MEA that forms stable carbamates, and then the overall reaction can be written like Reaction 5.[9]

$$CO_2 + 2RNH_2 \leftrightarrow RNHCOO^- + RNH_3^+ \quad (5)$$

MEA is a cheap amine to use in an absorption system. However, relatively high temperatures of at least 120°C are required for the regeneration. CCS systems with MEA as absorbent are therefore expensive and energy demanding, with the desorption column accounting for 70-80% of the operating costs. Investigations into other possible absorption mixtures and techniques are hence of great interest to make CCS more available.[9]

2.2 The pilot plant

The pilot plant investigated in this thesis uses an absorption mixture consisting of the amine AMP and the organic solvent DMSO. AMP is a sterically hindered alkanolamine and DMSO is a commonly used solvent in many laboratory applications. Their chemical structures are illustrated in Figure 3.

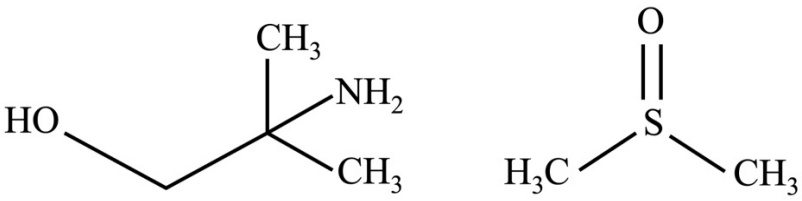

Figure 3. Chemical structure of 2-amino-2-methyl-1-propanol (AMP) to the left, and dimethyl sulfoxide (DMSO) to the right.

An advantage of using the combination of AMP and DMSO is that this mixture can be generated at temperatures between 70 and 90°C. This is lower than for conventional aqueous amine solutions like aqueous MEA which requires at least 120°C. This would allow for the possibility to use excess heat for this process step, which is usually available at many industrial sites. DMSO also has lower specific heat capacity than water and has a boiling point above the regeneration temperature, which is not the case for water when aqueous MEA solution is used. These factors reduces the heat required for the otherwise energy-intensive regeneration step.[9] Additionally, a carbamate that precipitates is formed when this mixture reacts with CO_2 as in Reaction 6-8.

$$CO_2(g) \leftrightarrow CO_2(sol) \tag{6}$$

$$CO_2(sol) + 2RNH_2(sol) \leftrightarrow RNH_3^+(sol) + RNHCOO^-(sol) \tag{7}$$

$$RNH_3^+(sol) + RNHCOO^-(sol) \leftrightarrow [RNH_3]^+[RNHCOO]^-(s) \tag{8}$$

When gaseous CO_2 encounters this mixture, it is first solved, according to Reaction 6. AMP then reacts with the solved CO_2 and a carbamate is formed, according to Reaction 7. Solid precipitation of the carbamate can then occur, according to Reaction 8. This carbamate could then be separated from the solution, creating an even richer CO_2-stream and a lean stream. By only letting the CO_2-rich stream go through the regeneration step, and leading the lean solution back to the absorption step, the energy demand could be reduced since less liquid needs to be heated.[9] The pilot plant thus utilizes a phase change absorption system and a typical flow sheet for this process is illustrated in Figure 4.

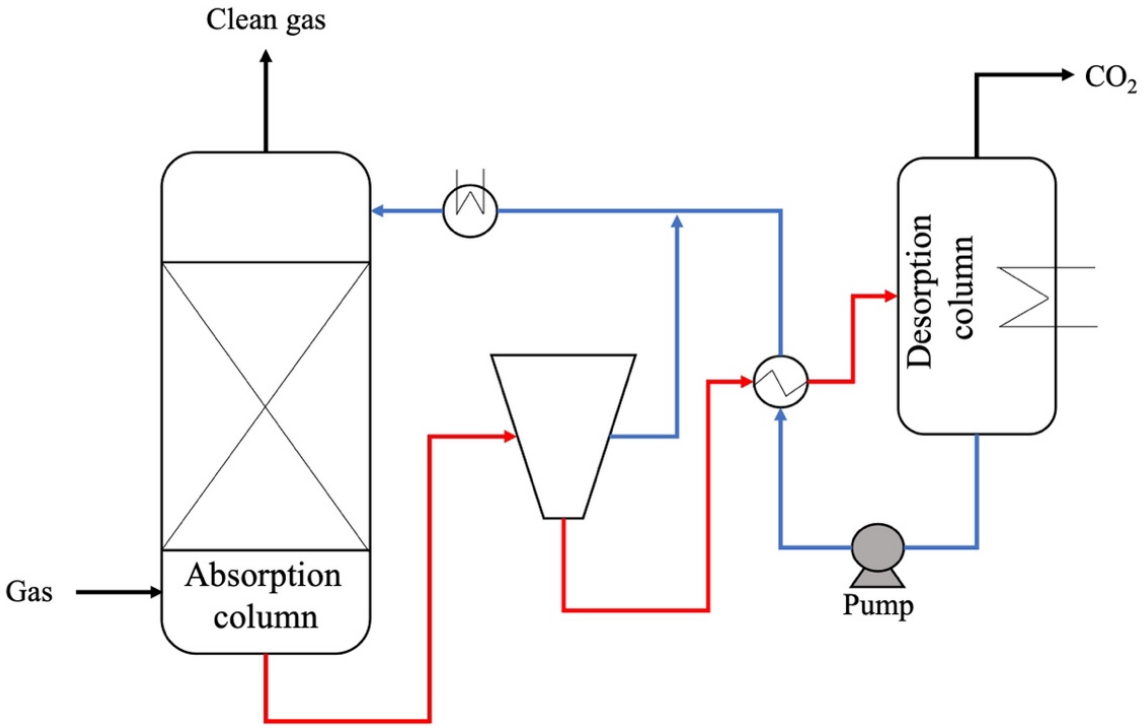

Figure 4. Schematic representation of a phase changing absorption process. The red lines indicate CO_2-rich solution, and the blue lines represent lean solution. This is a simplified flow sheet of the process used at the pilot plant.

2.3 Sampling methods

Amine absorption technologies for CCS are relatively mature and have been implemented in many industrial gas-cleaning processes. However, the effects of the potential emissions and their effects are not completely understood, and it is therefore important to carefully analyze the gas exiting these processes. Especially if the techniques are to be implemented at more sites and at larger scales. Some amines are for example toxic and could potentially also react to form new structures that may be more harmful than the original amine itself.[11, 14] AMP has also been suggested to inhibit ozone formation, indicating that it can enter chemical pathways in the atmosphere[10]. Since the pilot plant investigated in this thesis uses a novel combination for the absorption medium, the sampling and analysis procedures are extra important. Both liquid and gas samples were regularly taken from the pilot throughout its operating time at VEAB. The liquid samples were taken from installed taps placed at different streams in the pilot (the locations of the sampling spots can be seen in Figure 26 in Section 3.4). The gas samples were collected using two methods: the *impinger method* and the *cartridge method*.

In the impinger method, the gas sample is passed through a set of impingers like in Figure 5.

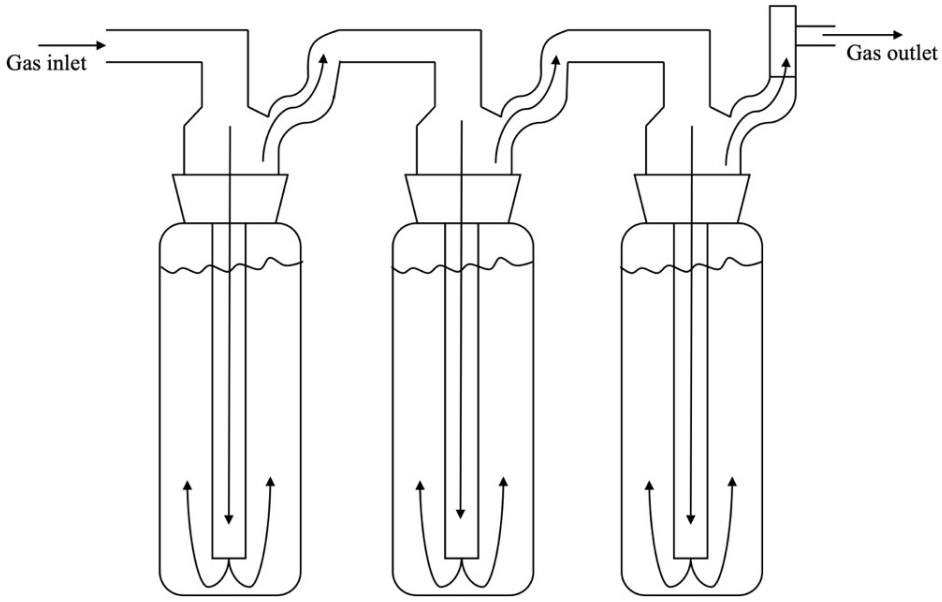

Figure 5. Illustrates an impinger setup with three impingers.

The impingers are filled with a liquid that will solve and stabilize the analytes of interest. To prevent carryover, multiple impingers in series are used and the amount of analyte in the gas is based on the amount found in all impingers.[15] If the last impinger in the series contains no analytes, the entire amount of analyte has been dissolved in the previous impingers. In this thesis, sulfamic acid and sulfuric acid were investigated as possible solvents since they were expected to solve and stabilize AMP and DMSO well when using the impinger method.[14] Both of these were solved in deionized water, with the dilution ratios presented in Section 3.1.

In the cartridge method, Thermosorb-N cartridges are used to collect analytes from a gas stream. These are then rinsed with a solvent to regenerate them and obtain the analytes.[15] Figure 6 shows a picture of the type of a Thermosorb-N cartridge that was used for sampling at the pilot plant. In this thesis, acetonitrile was investigated as a solvent since it was expected to solve AMP and DMSO well. The chemical structure of acetonitrile, sulfuric acid and sulfamic acid is displayed in Figure 7.

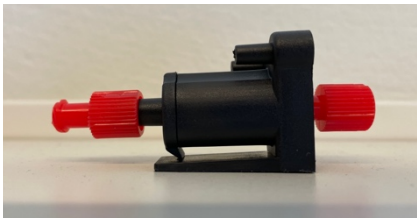

Figure 6. Picture of a Themosorb_N cartridge used at the pilot plant for gas sampling.

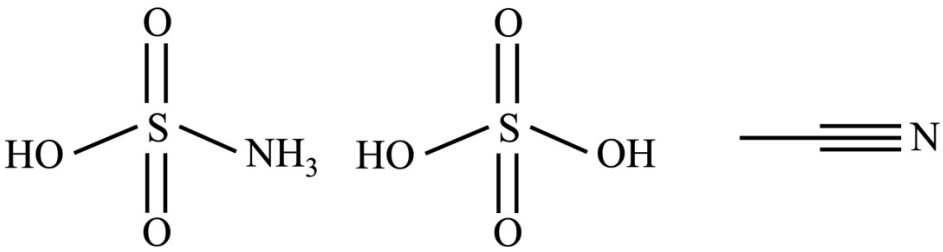

Figure 7. Chemical structure of sulfamic acid (left), sulfuric acid (middle) and acetonitrile (right).

2.4 The Chromatogram

Chromatography is a separation technique used in analytical chemistry to separate mixtures into their components in order to analyze them. The principle is that a *mobile phase*, containing the mixture that is to be separated, moves over a *stationary phase* which interacts with the analytes in the mixture. The stationary phase is usually placed in a column and the stronger the analytes interact with the stationary phase, the longer they stay in the column. Analytes with different tendencies to interact with the stationary phase will hence separate and can then be detected with a detector. The detector responses for each analyte can be used to create a *chromatogram*, which is the detector response plotted against time. The chromatogram can be used for qualitative identification and quantitative determination of individual analytes in the mixture.[16] Figure 8 shows a schematic representation of an arbitrary chromatogram.

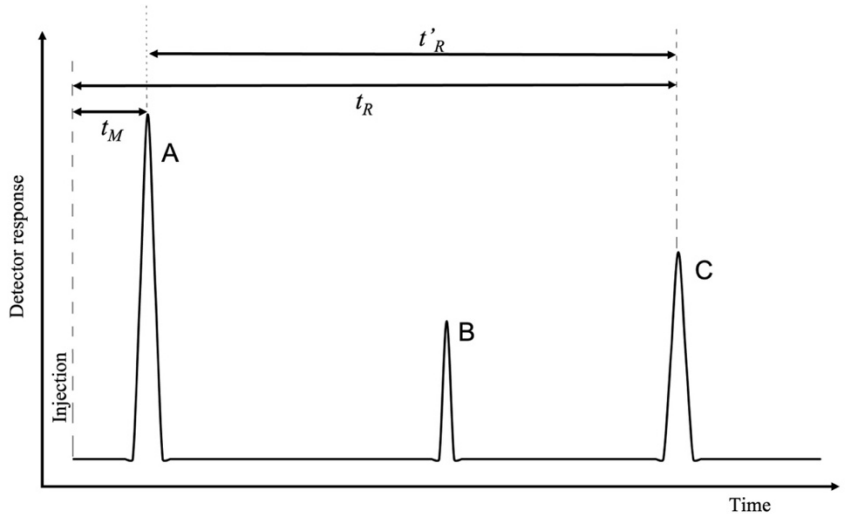

Figure 8. Displays an arbitrary chromatogram with three peaks, A, B and C. Detector response on the y-axis is plotted against time on the x-axis. t_M, t_R and t'_R represent the minimum time a component can travel through the column, the retention time and adjusted retention time respectively.

The chromatogram in Figure 8 shows three peaks which each represent one component of the injected sample. If there is no interaction between a component in the sample and the stationary phase, it elutes from the column at the shortest possible time, t_M, which is the case for component A. The time it takes from injection to the elution of analytes that do interact with the stationary phase is referred to as *retention times,* t_R. The *adjusted retention time,* t'_R, is the time difference between retention time and the shortest possible retention time.[16, 17]

$$t'_R = t_R - t_M \tag{1}$$

Both the retention times and adjusted retention times can be used to identify components in the mixture and measure the efficiency of separation between two peaks. There are different ways in which separation can be measured. One is by calculating the *separation factor,* α_s. The separation factor for peaks B and C in Figure 8 can be calculated from their adjusted retention times according to Equation 2.[16, 17]

$$\alpha_s = \frac{t'_{R,C}}{t'_{R,B}} \tag{2}$$

This value can give an indication of the separation and can be useful for identifying peaks when different flows of carrier gas are used since it is independent of the flow rate. The higher value of the separation factor, the better the separation. It should however be noted that this factor does not take the widths of the peaks into account, which can give misleading results. Two peaks that interfere with each other might still give a high separation factor if the peak tops appear far apart. A more accurate way of measuring the efficiency of separation, that take the widths of the peaks into account, is instead to calculate the *resolution,* R_s. Resolution can be determined with Equation 3.[16]

$$R_s = \frac{t_{R,C} - t_{R,B}}{w_{av}} = \frac{0.589\left(t_{R,C} - t_{R,B}\right)}{w_{1/2av}} \tag{3}$$

Where w_{av} is the average of the two peak widths and $w_{1/2av}$ is the average of the peak width at half their peak heights. Usually, the width at half the peak height is used to measure resolution since it is easier to measure than the baseline width. The resolution is generally considered sufficient for quantitative analysis when $R_s > 1.5$, which indicates that *baseline resolution* has been achieved. Baseline resolution means that the signal reaches the baseline in between the peaks.[16] It should however be noted that Equation 3 assumes ideal Gaussian peak shapes, which is not always the case in real chromatograms.

2.4.1 Qualitative analysis using chromatograms

Qualitative analysis is performed by comparing the retention time of an analyte from different samples, usually a standard sample with known composition and one unknown sample. For example, if two analyses are performed with the same conditions and method settings, the retention times of the same analyte should match in the two generated chromatograms[16], as in Figure 9.

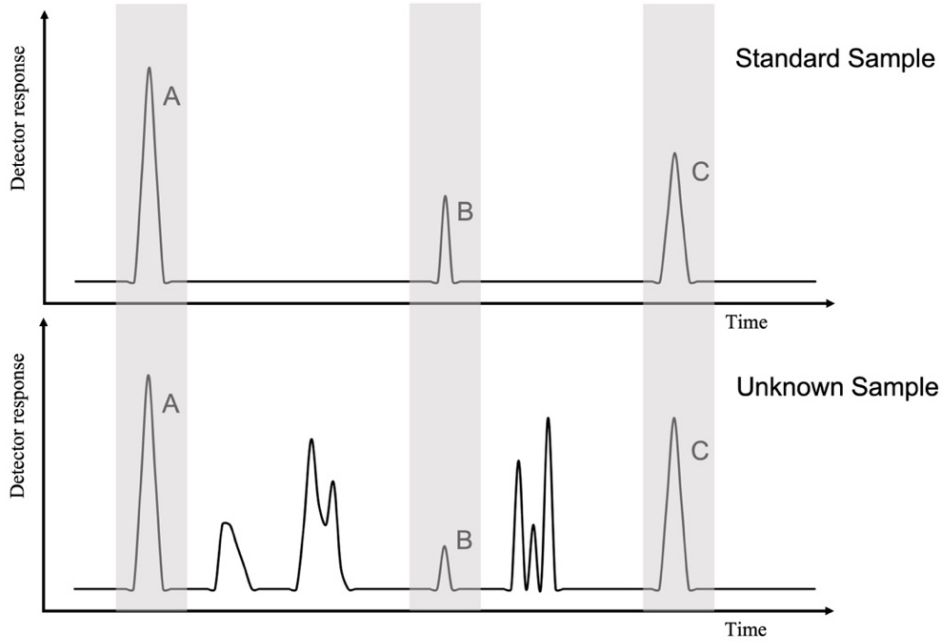

Figure 9. Shows how qualitative analysis is preformed using chromatograms. If the analyses are performed with the same conditions and method settings, the retention times should match for the same analytes in a standard sample and a sample with unknowns.

The retention times should be independent of analyte concentration and other varieties in sample composition, like in Figure 9. Using a standard sample that only contains the analytes of interest in the solution to compare with other chromatograms is hence an efficient way of identifying peaks.[16]

2.4.2 Quantitative analysis using chromatograms

Quantitative analysis is performed by measuring the area or height of the peaks in the chromatogram. The height can be used for peaks with very sharp shapes but for most applications, the peak area is more suitable. The peak area should be proportional to the amount of analyte that reaches the detector. By comparing the measured peak area to a standard sample with a known amount of analyte, the amount in the unknown sample can hence be determined using the linearity between peak area and amount of analyte.[16] Figure 10 shows a visual representation of this.

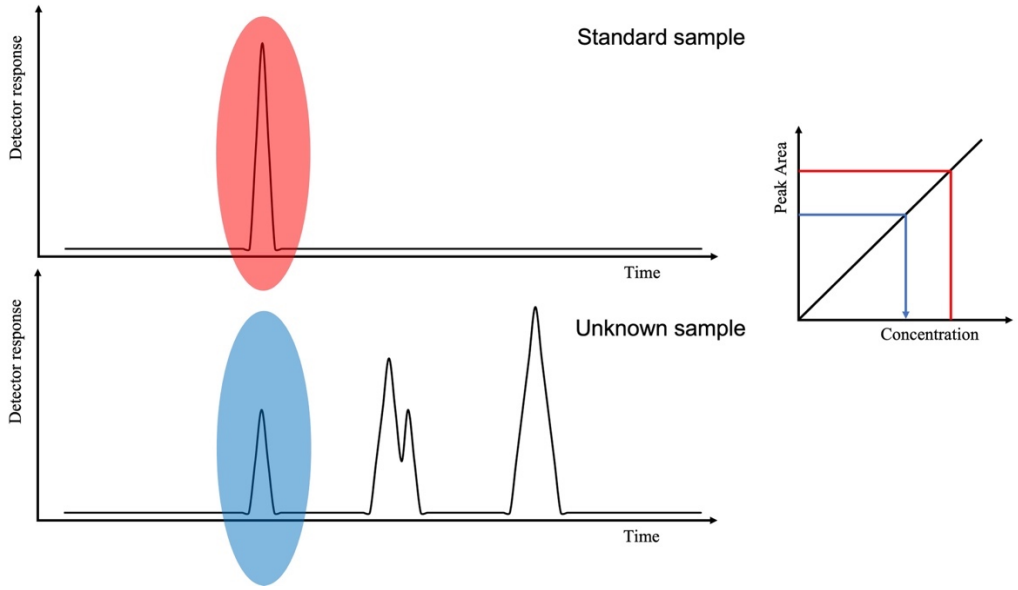

Figure 10. Shows how quantitative analysis can be performed by comparing the peak size of the unknown sample with the peak size of a standard sample with known concentration.

A common quantitative analysis method that utilizes this principle is the *external standard method.* In this method, several standard samples with different concentrations of analytes are prepared and analyzed. Their responses are then plotted against their concentrations to generate a calibration curve. The linear regression of this external calibration curve can then be used to determine concentrations of unknown samples[16], as shown in Equation 4.

$$y = kx + m \leftrightarrow x = \frac{y - m}{k} \tag{4}$$

Where x is the concentration of the unknown sample (on the x-axis), y is the peak area (on the y-axis), k is the slope of the calibration curve and m is the intercept between the calibration curve and the y-axis.

Another quantitative analysis method is the *internal standard method*. In this method an internal standard is added to the unknown sample. The internal standard should be a compound of

known concentration that is not already present in the sample. The concentrations of the analytes are then calculated based on the relation between the peak area ratio and the concentration ratio of the analyte and internal standard[16], according to Equation 5.

$$\frac{A_x}{A_i} = F\frac{[x]}{[i]} \leftrightarrow [x] = \frac{[i]}{F}\frac{A_x}{A_i} \tag{5}$$

Where A_x is the area of the analyte peak, A_i is the area of the internal standard peak, *[x]* is the unknown concentration of the analyte, *[i]* is the concentration of the internal standard and F is the response factor. The response factor accounts for the difference in detector response for each component and needs to be determined before the analysis. This can be done by preparing a mixture with known concentrations of analyte and internal standard to find out their relative response. However, to average out some possible experimental errors, a multipoint calibration curve with varying concentration ratios is preferred. The peak areas should have a linear response if plotted against the concentration ratios and the slope of the generated calibration curve is hence the response factor. The benefit of using this method is that concentration ratios are largely independent of injection volume and variations in detector response between different runs. The external calibration curve is dependent on these parameters remaining the same between runs, which might not always be the case in practice. The internal standard method is, however, more time-consuming and it requires a suitable internal standard to be found for each analysis method. The internal standard should preferably have a similar chemical structure as the analyte, since it would more likely behave similarly if the analysis parameters change slightly. However, it needs to be different enough to elute with a different retention time and with sufficient separation from other analytes.[16]

2.5 Gas Chromatography (GC)

Gas chromatography (GC) was the analysis technique used in this thesis to develop the analysis methods and to analyze the samples from the pilot plant. GC is a common chromatographic technique used in analytical chemistry for separating and analyzing organic compounds. The principle is that the analyte is injected into the gaseous mobile phase, called the *carrier gas*, and passed through a column that contains the stationary phase. The stationary phase interacts with the analytes based on their boiling point and polarity, which separates them and enables individual analysis of the compounds.[16] Figure 11 shows a schematic representation of a typical gas chromatographic setup.

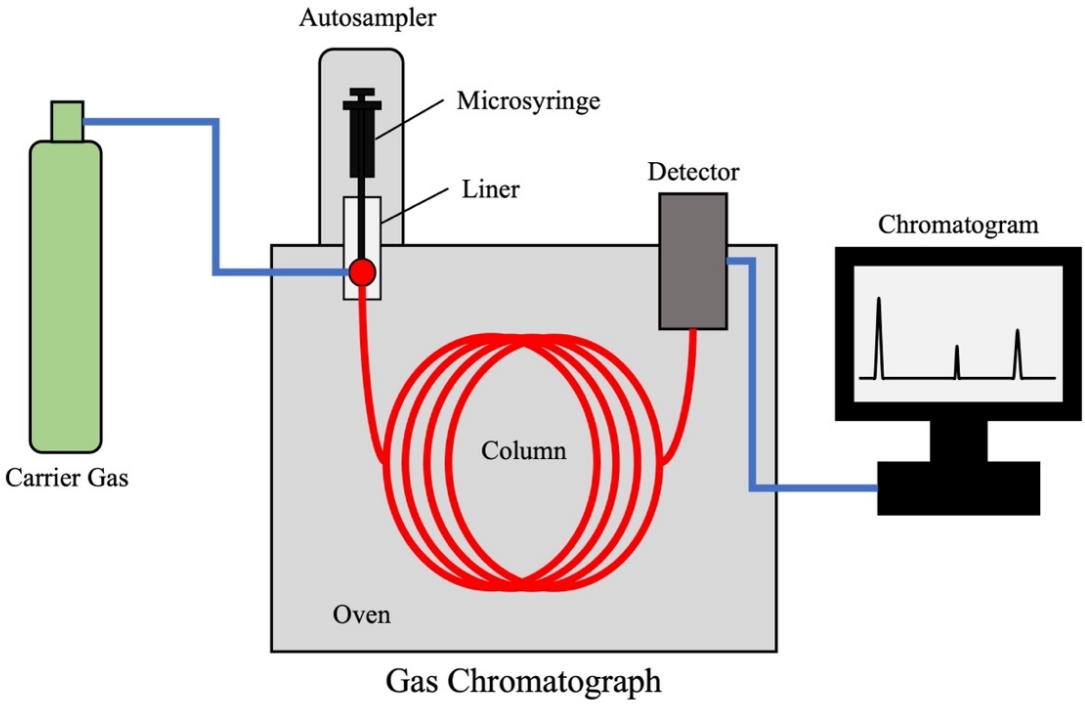

Figure 11. Schematic representation of a typical gas chromatographic set up.

The gaseous or liquid sample is usually injected into the gas chromatograph through an autosampler, where it is heated and rapidly evaporated. It is then transported with the carrier gas through a column which is placed in a temperature-controlled oven. The components in the sample will interact differently with the stationary phase in the column, depending on the type of column and oven temperature. This leads to variations in the amount of time analytes spend in the column, resulting in different elution times for each of them. The separated analytes are then passed through a detector that generates a chromatogram, which can be used for quantitative and qualitative analysis.[16] When selecting settings for a GC analysis, it is important to understand the concepts of the different parts of the GC set up and how they can affect the chromatogram. The following sections gives more detailed descriptions of these parts and what role they play for the results of the analyses.

2.5.1 Column

There are two types of columns used in GC. Either *open tubular columns* or *packed columns*, with the former being the most commonly used. Packed columns are usually made of stainless steel and are filled with small solid particles that make up the stationary phase.[16, 18] Open tubular columns are instead typically made of fused silica with a layer of polyimide on the outside that can withstand the high temperatures from the oven. Open tubular columns can also be made of deactivated stainless steel which makes them less sensitive to breakage. The inside of the tube is coated with a thin layer of the stationary phase which can either be in liquid phase (wall-coated column) or in solid phase (porous-layer column).[16, 19] It is the molecular interactions between the stationary phase and the mobile phase that enable the separation of analytes in the sample. The chemical structure of the stationary phase is hence of great importance for the analysis and the choice follows the rule of *like dissolves like.* Polar columns are preferred for polar solutes and non-polar columns are preferred for non-polar solutes. For polar columns, the elution order of the analytes is determined by their polarity. More polar compounds will have

a stronger interaction with the stationary phase compared to less polar compounds and will elute from the column at a later stage. The elution order in a non-polar column is instead governed by the volatility of the analytes, where compounds with lower boiling points will elute before compounds with high boiling points.[16]

The stationary phase is usually attached to the silica surface with covalent bonds to prevent stationary phase from dethatching from the column. A column that loses stationary phase in this way is called a bleeding column and can cause the background noise of the detector to increase, which will make the analyze less sensitive. However, as columns age, and by being constantly exposed to high temperatures, this is difficult to prevent. Since higher temperatures tends to increase bleeding, it is important to keep the temperature program of the oven below the maximum operating temperature of the column. It is also important to use a carrier gas with high purity since oxygen tends to oxidize the stationary phase, causing it to bleed as well.[16]

When selecting a column, the ratio between stationary phase film thickness and column diameter should also be considered. A narrow column with thin film thickness gives better separation than a wider column with thicker film, but at the expense of capacity. Thin and narrow columns do not retain compounds with low boiling points that well and the thin film thickness makes active sites on the silica more likely to be exposed. A narrow column with a thick film is therefore usually a good compromise.[16]

2.5.2 Detector

The detectors available for gas chromatographic analyses can be separated into two broad categories: *universal detectors* and *selective detectors*. Universal detectors respond to all analytes in the sample, excluding the carrier gas. Selective detectors instead only respond to a specific type of analyte which could simplify the chromatogram and reduce potential matrix effects.[16]

The *flame ionization detector* (FID) is a commonly used detector and the one used for all analyses in this thesis. It has a selective response to most organic compounds[20]. The principle of the detector is that the eluting sample is burned in a flame generated by a hydrogen and air stream. The carbon atoms form CH radicals in the flame, which then form CHO^+ ions and electrons according to Reaction 9.[16]

$$CH + O \rightarrow CHO^+ + e^- \quad (9)$$

The produced ions initiate a current which is measured with an electrometer and amplified into a proper voltage. This voltage is then converted into a digital signal which is displayed as a chromatogram. Not all carbon atoms form ions, but the rate of ion formation is proportional to the number of carbons entering the detector. The response is hence based on mass rather than concentration. Since the compounds are burned, the sample is lost in the analytical process. Nitrogen is usually used as a makeup gas to optimize the detector performance.[16]

2.5.3 Sample injection

Both liquid and gas samples can be analyzed using gas chromatography. For liquid samples volumes around 1 µL are injected and for gas samples volumes between 10 µL up to 5 mL. The injection can be performed manually, but many machines provide an autosampler that injects a preprogrammed volume automatically. First, the sample is taken from a vial with a

microsyringe, which is then injected into a heated *injector port* where it is rapidly evaporated.[16] Figure 12 displays the setup of an injector port.

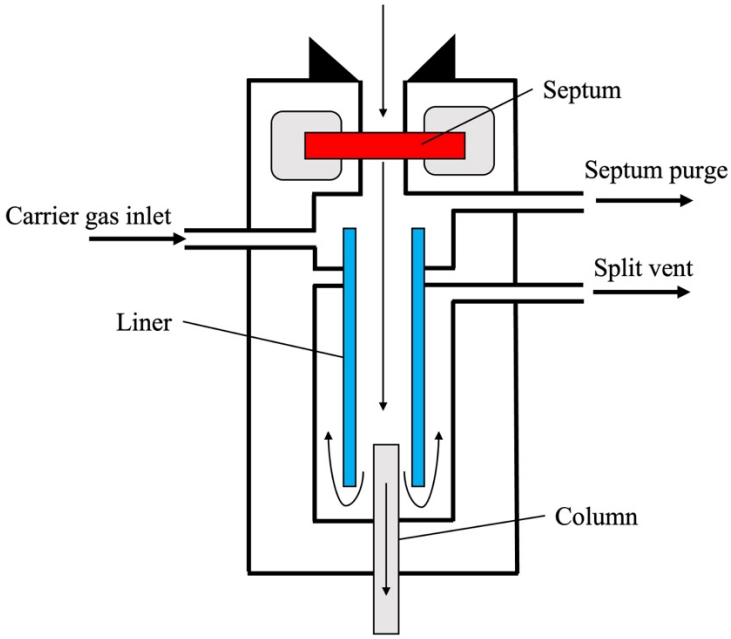

Figure 12. Illustration of an injector port. The microsyringe penetrates the septum at the top and releases the sample into the liner before it eventually enters the column.

The injector port consists of a rubber septum, which prevents leakage, and a glass liner, which filters out nonvolatile impurities. Both the septum and the liner lose performance over time and need to be replaced eventually. For an autosampler, the septum should be replaced after around 100 injections.[16]

Depending on the concentration of the analyte of interest in the sample, either *split-* or *splitless injection* can be used as the injection technique. In split injection, only a fraction of the sample taken from the vial is introduced into the column and the rest is led to a waste vent. This is preferred for more concentrated samples to not overload the column. The ratio of the amount of sample entering the column and the amount of sample going to waste is called the *split ratio* and is an important parameter when developing a chromatographic method that gives optimal peak shapes in the chromatogram. The split ratio can vary from 1:1 up to 500:1, where lower ratios give larger peaks and smaller concentrations can hence be detected. However, a low ratio can also result in broader and more asymmetric peaks. Higher ratios make the analytes enter the column faster and with better precision on the amount of sample that enters. This gives sharper and more stable peaks, but lower concentrations are not able to be detected. For less concentrated samples, the splitless injection might be a more suitable alternative. The principle is similar to split injection, with the difference that the whole sample in the microsyringe is transferred into the column. It is also a slower injection where the sample spend more time in the inlet and the injector temperature need to be lower than for split injection to prevent it from decomposing. When the sample eventually enters the column, a small amount is always lost and flushed through the waste vent. This makes splitless injection slightly less sensitive compared to split injection. Since more sample is loaded on the column when splitless injection is used, the detection limit can be enhanced, but it also gives broader peaks.[16]

2.5.4 Carrier gas

The carrier gas is the mobile phase that carries the injected sample through the column. The three most common carrier gases used in GC are helium, hydrogen, and nitrogen. They all have pros and cons when it comes to performance, speed of analysis, price, availability, and analytical compatibility. Helium shows great compatibility with most detectors, but nitrogen gives lower detection limits when flame ionization detectors are used. Both nitrogen and hydrogen are less expensive than helium and can be produced on-site.[21] How the efficiency of the gases is measured can be explained using the V*an Deemter equation*, see Equation 6.

$$H = A + \frac{B}{u_x} + Cu_x \tag{6}$$

Where u_x is the linear velocity and H is the plate height. In GC, plate height is used as a measurement of the efficiency of the column[22]. A low plate height-value provides sharper peaks and better separation.[16] The A term is a constant that accounts for the effects of the multiple paths the flow can take in a packed column. Since the flow in an open tubular column typically flows linearly, this term is only applicable to packed columns. The B term accounts for the longitudinal diffusion of solutes in the mobile phase and the C term accounts for the resistance to mass transfer. The combined contribution of all the terms can be seen in the Van Deemter curve, shown in Figure 13, where plate height is plotted against the linear velocity of the carrier gas flow.[22]

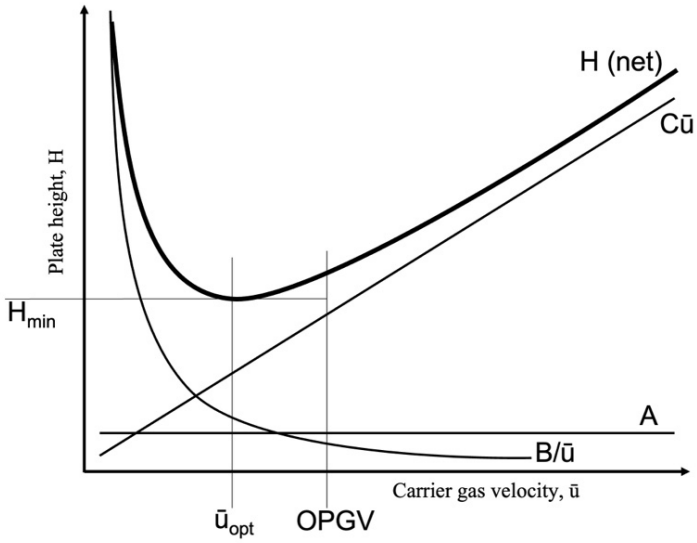

Figure 13. Van Deemter curve demonstrating the combined effects of the A, B and C terms in the Van Deemter equation. On the y-axis is the plate height, H and on the x-axis is the carrier flow velocity, ū. The minimal plate height, H_{min}, at which the conditions are the most efficient, gives the optimum velocity, $\bar{u}_{opt}$, and optimal practical gas velocity, OPGV (~$2\bar{u}_{opt}$).

At lower velocities, B is the dominant term since more solute diffusion occurs in the mobile phase at low flows. At higher velocities, C is instead the dominant term since higher flows give solutes less time to reach equilibria, giving rise to higher mass transfer resistance.[22] Figure 13 also displays the optimal efficiency, $\bar{u}_{opt}$ at minimal plate height, and the optimal practical gas velocity (OPGV). OPGV is usually defined as double the optimal velocity and is usually preferred since it provides faster analysis time without losing a considerable amount of

efficiency.[22] The efficiency of the carrier gases can be compared by plotting the respective Van Deemter curves for the different carrier gases in the same plot, as in Figure 14.

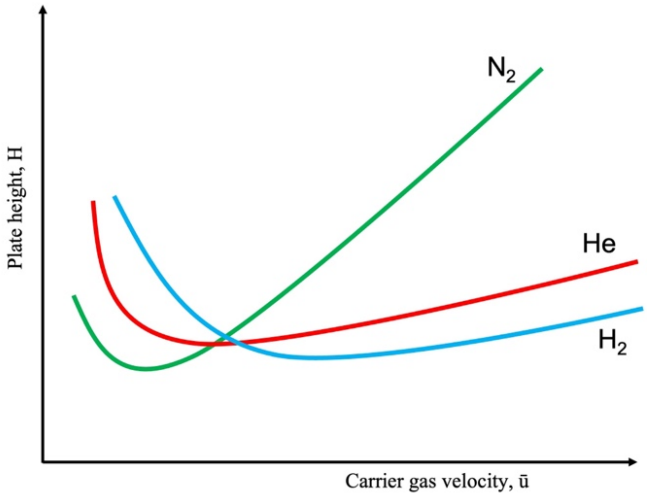

Figure 14. Van Deemter curves for nitrogen (green), helium (red) and hydrogen (blue).

The velocity that provides optimal efficiency follows the increasing order $N_2 < He < H_2$. This means that hydrogen can carry out the fastest analysis and the velocity can be increased with only small losses in efficiency. Hydrogen is therefore considered the most optimal choice for many applications. However, the explosive nature of hydrogen necessitates extra measures regarding safety, since a concentration of 4% hydrogen in air can lead to an explosion[23]. Nitrogen has the lowest optimal velocity, which results in the slowest analysis, and there is not much room to increase it without losing considerable efficiency. The reason that hydrogen and helium give better efficiency at higher velocities is that solutes diffuse faster through hydrogen and helium than through nitrogen. The faster a compound diffuses in the mobile phase, the smaller is the resistance to mass transfer and the less dominant is the *C* term in the Van Deemter equation. Nitrogen is however an efficient carrier gas since it provides the smallest plate height at its optimal velocity, see Figure 14.[21]

Sometimes the carrier gas flow can be too low to achieve the best detector performance. This can be solved by introducing a *makeup gas* after the column, but before the detector. The most suitable makeup gas may be a different gas than the carrier gas and depends on the type of detector. The purity of the carrier gas is also of importance for a high-quality analysis. Impurities can cause baseline noise (see section 2.6.2) and might interact with analytes or active sites on the stationary phase. Traces of oxygen and water in the gas can for example cause oxidative degradation of the stationary phase, which gives wider peaks, tailing peaks and shifts in retention time.[16]

2.5.5 Temperature and Pressure

GC analysis can be performed either under *isothermal conditions*, where the temperature in the oven is kept constant, or with a *temperature program,* in which the temperature is increased gradually throughout the analysis. A temperature program offers advantages like decreased retention time and sharper peaks for late eluting compounds. The answer to why this is can be found by looking closely at the interactions between the analytes and the stationary phase. As analytes move along the column, they are constantly in an equilibrium state with the stationary

phase and the mobile vapor phase. By raising the temperature, the vapor pressure of each analyte is also increased which moves the equilibrium towards the vapor phase.[16] The relation between the temperature and vapor pressure of a compound is governed by the *Clausius-Clapeyron equation*, see Equation 7.

$$\ln P_{vap} = -\frac{\Delta H_{vap}}{RT} + C \tag{7}$$

Where P_{vap} is the vapor pressure of the compound, ΔH_{vap} is the enthalpy of vaporization of the compound, T is the temperature, R is the gas constant and C is a constant specific to the compound.[16, 24]

If a sample contains several compounds with different boiling points and the analysis is performed under isothermal conditions, there is a risk that low boiling-point compounds interact so weakly with the stationary phase that they elute at similar times. This can give insufficient separation and poor peak shapes. Moreover, high boiling-point compounds might interact to such a large degree that they do not even elute at all within the time of the analysis program, and this is referred to as the *general elution problem*. This can be solved by using a temperature program. It can be seen from the Clausius-Clapeyron equation, that a linear increase in temperature give rise to an exponential increase in vapor pressure. The retention time for late eluting peaks can hence be substantially shortened and give an even spread of peaks in the chromatogram.[16] Figure 15 shows the difference between two chromatograms for the same sample, one performed isothermally and one with a temperature program.

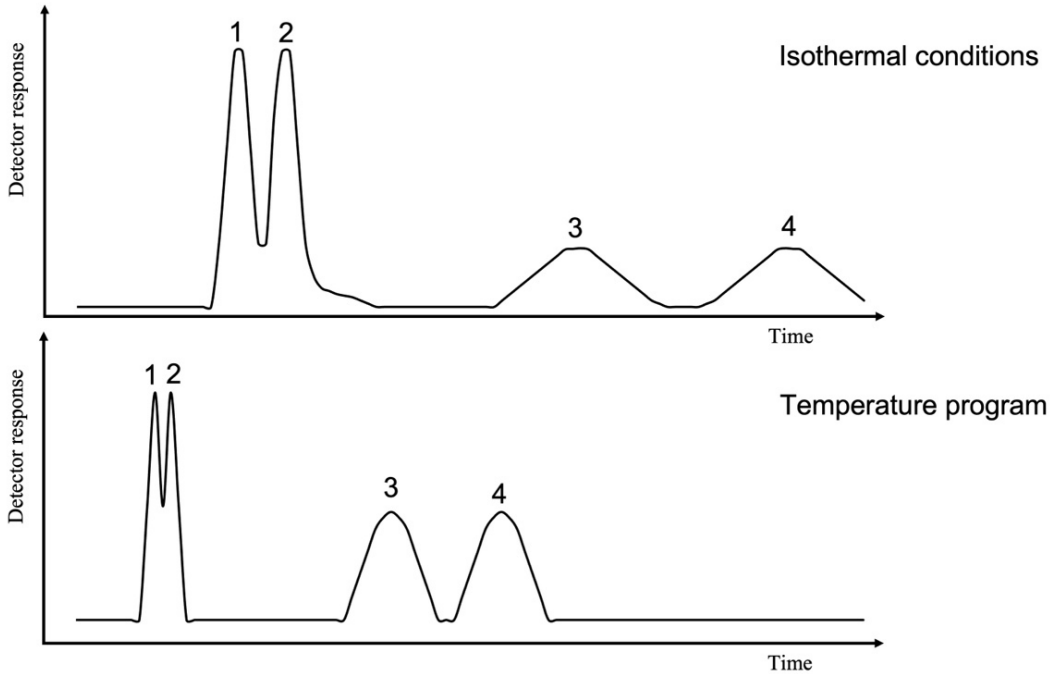

Figure 15. Shows two chromatograms for the same sample. The chromatogram at the top has been run with isothermal conditions and chromatogram at the bottom has been run with a temperature program.

Figure 15 shows that a temperature program can decrease the retention times for late eluting peaks. It also shows that the peak shapes of the late eluting compounds become sharper when run with a temperature program. This is because the temperature program enables strong

retention of the compounds by having a low initial temperature compared to the boiling point of the compounds. Most compounds are hence retained in the head of the column until the temperature is high enough for the compound to reach sufficient vapor pressure after which they start moving down the column. This was explained by Giddings, who approximated the relationship between the rate of zone mitigation and the increase in temperature as a step function, allowing one to approximate each step as an isothermal run. Furthermore, the strong initial retention can prevent a large fraction of the diffusion occurring in the stationary phase, which contributes to the sharper peak shapes.[25]

2.5.6 Sample preparation

Cleaner samples give cleaner chromatograms and sometimes preparation of the samples is needed before it can be analyzed with GC. This could include a variety of steps and procedures. For instance, it might involve extracting the analytes from a complex matrix to simplify the chromatogram or spiking the sample with analyte to get into sufficiently high concentrations for the analytical method. It could also involve filtration to remove interfering compounds or even chemically change the analytes into something that better suits the method. All this depends on the type sample that is to be analyzed.[16]

2.6 GC Trouble shooting

There are a fair number of problems that can arise during a GC analysis. This section discusses a few common problems, their potential causes and how to solve them.

2.6.1 Ghost Peaks and Carry over

Ghost peaks are peaks that appear at positions in the chromatogram where a peak is not to be expected. This is illustrated in Figure 16. A peak does not spontaneously emerge, instead any unexpected peaks must originate from unexpected components introduced somewhere in the process. This could for example be contamination that is introduced with the sample. If this is the cause, sample preparation steps should be looked over and the sample or solvent might need to be purified. Another possibility is that the contamination is introduced at the inlet. This might be from contamination in the needle, the liner, or the septum. All of these should be cleaned and replaced regularly to avoid this problem. Unexpected peaks could also come from semi-volatile components from previous runs that did not elute within the analysis time, so-called carryover. These components can be eluted by either running the program without injection, *bake-out*, or injecting pure solvent into the column. It is quite common to include solvent rinses in between samples in a sequence of samples and to end the sequence with a bake-out to avoid carryover.[26]

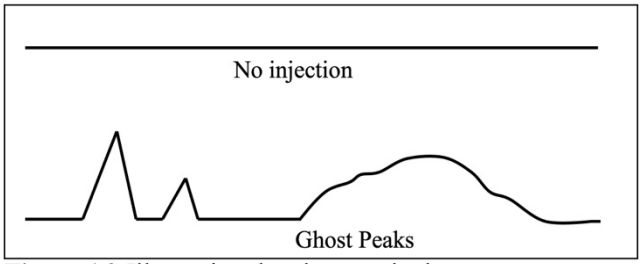

Figure 16. Illustration the ghost peak phenomena.

2.6.2 Extensive Baseline Noise

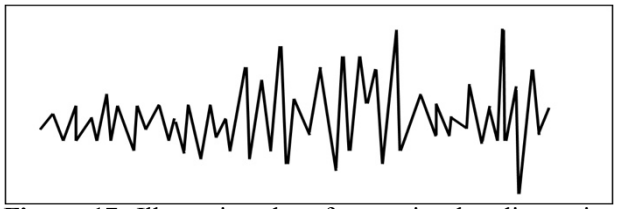

Figure 17. Illustration the of extensive baseline noise phenomena.

It is not uncommon that baselines have small fluctuations in signal intensity during the analysis, but too extensive noise could influence the results of the analysis. This can be caused by injector or column contamination and could be solved be cleaning the needle regularly and potentially bake-out the column. It could also be caused by detector contamination, which can be difficult to notice since it usually manifests as a gradual increase in baseline noise over time. Regular cleaning of the detector can solve this problem. Impurities in the carrier, makeup and detector gas are another possible cause, as well as unsuitable gas flows. Cleaner gases with optimized flows result in better chromatograms. Improper column installation, in which the column is inserted too far into the detector, might also cause baseline noise and reinstalling the column should resolve the problem. Aging equipment is also a common cause, especially the detector, the septum and the column. Replacing these will likely give more stable baseline noise.[26]

2.6.3 Baseline Instability or Disturbances

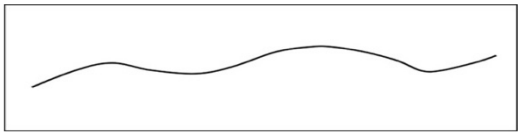

Figure 18. Illustration of an unstable baseline.

An unstable or drifting baseline as in Figure 18, could be caused by injector or column contamination. It can also be related to improper equipment settings. The detector can for example be unstable, which is common when it is newly installed. Letting the detector stand untouched and stabilize should help, sometimes for as long as 24 hours. It can also be improper gas flows that causes disturbance. Some temperature programs can even benefit from changing the gas flows during the run.[26]

2.6.4 Fronting Peaks

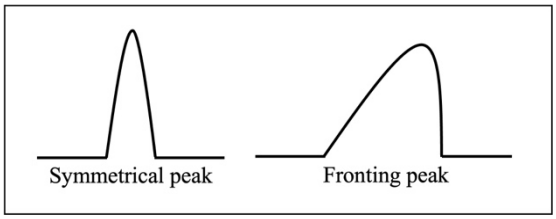

Figure 19. Illustration of the difference between a symmetric and a fronting peak.

Fronting peaks occur when the shape of peaks resembles the example depicted in Figure 19. This is not ideal for analysis and the most common cause is column overload, when too much analyte is introduced into the column. The simplest solution is to reduce the amount of analyte injected into the column by decreasing the injection volume, diluting the sample or increasing the split ratio. Fronting peaks could also be caused by the injection technique if manual injection is used, where switching to an autosampler should help. The solvent could also play a part in fronting peaks. If the analyte is very soluble in the solvent, it might be necessary to change the solvent. As with many other GC problems, it could also be the column that is improperly installed.[26]

2.6.5 Tailing peaks

Tailing peaks occur when the shape of peaks resembles the example in Figure 20. This could be caused by column contamination or poor column installation. Reinstalling, trimming or rinsing the column are some common measures to solve this. If the sample contains active compounds, it could be that the column activity has decreased, which is irreversible, and the column would have to be replaced. Tailing peaks could also occur if multiple solvents with different polarities are used and usually give more tailing for peaks eluting close to the solvent. As for fronting peaks, it could also be that too much analyte is injected and that the split ratio is too low. One should also keep in mind that some active compounds always tail, which is especially common for amines and carboxylic acids.[26]

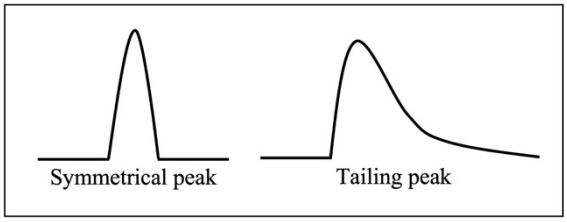

Figure 20. Illustration of difference between a symmetrical peak and a tailing peak.

2.6.6 Split peaks

Split peaks are peaks that gives multiple tops where only one analyte is expected to be present, as illustrated in Figure 21. This problem can arise from the injection technique and the risk is reduced by using an autosampler. It can also be caused by poor column installation. If more than one solvent is used it could also be a too large difference in polarity between them, which causes the split. Sample degradation in the injector is a common cause as well, which could be fixed by decreasing the injector temperature or using on-column injection. Another potential explanation could be that the temperature program is not compatible with the components in the sample and one would have to find a more suitable program.[26]

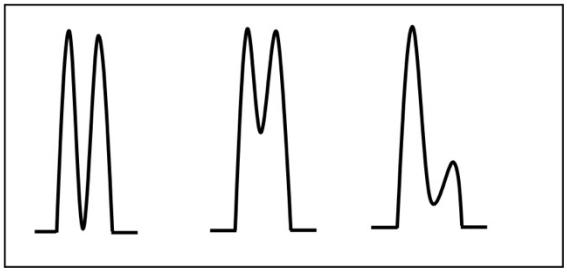

Figure 21. Illustration of three types of peaks that all shows split peak behavior.

2.6.7 Retention Time Shift

Figure 22 illustrates two chromatograms from the same sample where there has been a shift in retention times. There are many reasons why retention times may shift. It could for example occur if the carrier gas velocity is changed either by a leakage or by the GC method settings. This is characterized by all peaks shifting in the same direction and to the same extent. If all peaks are not affected in the same way, it could be that the column temperature has changed. It could also be something more drastic, like a change in column dimension or a large change in analyte concentration. If there is also a change in peak size, it is likely due to a leakage in the injector or in the septum.[26]

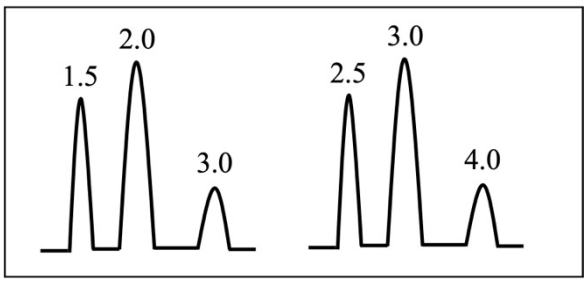

Figure 22. Illustration of two chromatograms from the same sample with shift in retention times.

2.6.8 Change in Peak Size

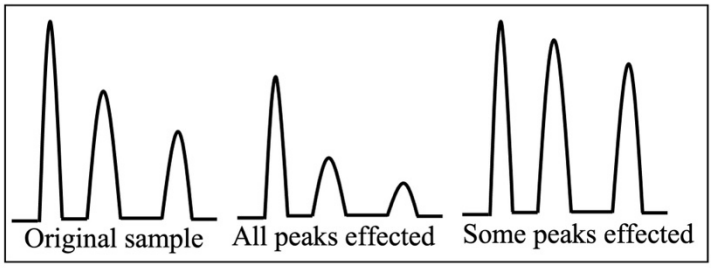

Figure 23. Illustration of the effects of peak size change, comparing chromatograms for the same sample in which all peaks are affected in the middle and only some to the right.

Change in peak size between runs of the same sample is a common occurring problem in gas chromatographic analyses and there are many possible causes. The first step involves examining whether anything has changed in the settings of the method, like a change in split ratio or injection volume. A different split ratio might not affect all peaks the same way and a change in injection volume does not always show a linear change in response. Another possible cause could be that the sample itself has changed. This could for example be because of degradation or evaporation of compounds, or because of a difference in temperature or pH between the runs. If the problem is not related to the sample, it could instead be an error with the equipment. A leak in the syringe can cause variations in the amount of sample that is injected into the column and affect the peak sizes. It can also be caused by contamination from the column, liner or injector. It is recommended to regularly clean the injector and replace the liner regularly to prevent this problem. Regularly rinsing the column with pure solvent could also help to reduce the risk of contamination. If there is contamination in the column, it is likely placed in the inlet of the column and it could therefore help to trim it by removing a part of the column front using a special cutting blade. It should however be noted that this will likely change the retention times of the analytes slightly. If only peaks from active compounds in the sample are affected, the change in peak size can be because the column activity has changed. This is irreversible and the column has to be replaced if this occurs.[26]

2.6.9 Loss of Resolution

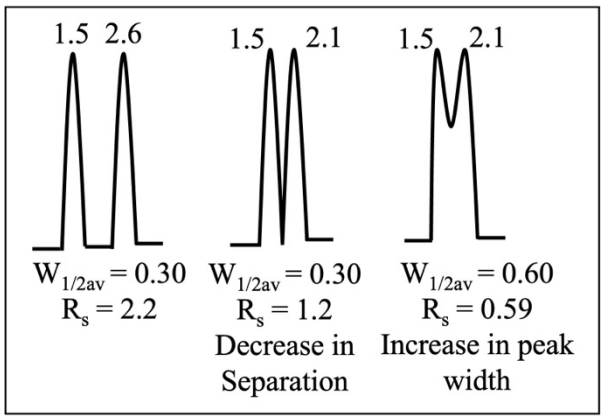

Figure 24. Illustration of three chromatograms from the same sample, the one in the middle has lost resolution due to decrease in separation and the one to the right due to increase in peak width.

Loss of resolution can either be due to a decrease in separation or an increase in peak width, see Figure 24. A decrease in separation could be caused by a change in column temperature, dimension or phase and would affect all peaks in the chromatogram. It could also be because of the co-elution of multiple peaks. This would require a more suitable temperature program that would allow for more efficient separation. An increase in peak width can be due to a change in carrier gas velocity, which would likely also affect the retention times. As for a change in peak size, it could also be linked to column contamination, in which case trimming or rinsing the column could solve the problem. Since peaks typically become wider with increasing analyte amount and concentration, any change in injector settings or sample concentration could also cause a loss of resolution. For splitless injections, another possible cause could be improper solvent. This could be solved by lowering the oven temperature or

switching to a better solvent with a polarity that better matches the polarity of the analytes and stationary phase.[26]

3 Materials and Methods

The working procedures in this thesis can be summarized into a few broad steps, which are summarized in Figure 25 below.

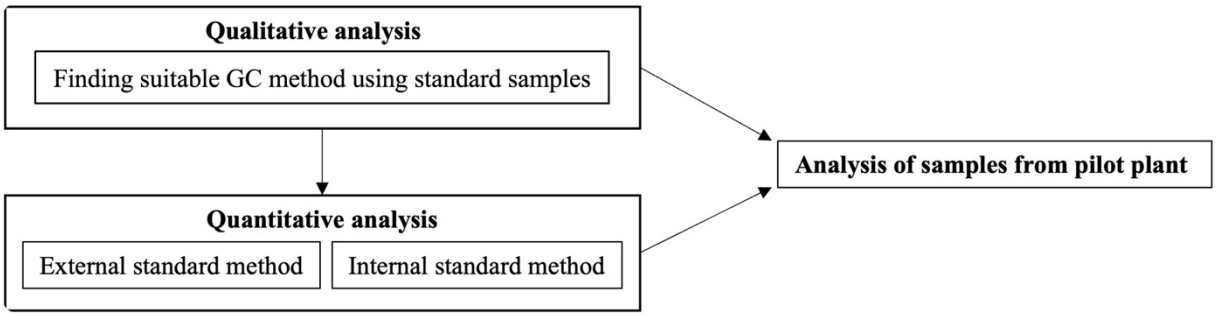

Figure 25. Displays an overview of the steps carried out in the method section of this thesis. The qualitative and quantitative analyses were first done on samples prepared in the lab and the methods and solvents that worked the best were later used to analyze samples from the pilot plant.

In the first step, qualitative analysis was performed on standard samples prepared in the lab to investigate if the analytes (AMP and DMSO) could be identified with GC when solved in the different solvents (acetonitrile, sulfamic acid and sulfuric acid). This included the preparation of a variety of standard samples and finding suitable method settings for the GC analysis program. In the next step, quantitative analysis was performed on samples prepared in the lab, with the solvent and GC method settings that showed the most promising results in the qualitative analysis. Both the external standard method and the internal standard were investigated (the principles of these are explained in Section 2.4.2). More detailed descriptions of how the qualitative and quantitative analyses were performed on the lab samples are provided in Sections 3.2 and 3.3. The methods that showed the most promising results for the lab-samples were then used to analyze samples taken at the pilot plant. These methods were validated based on selectivity, linearity and precision, as described in Section 3.5.

3.1 Equipment and Chemicals

The main chemicals used for making the lab samples were *2-amino-2-methyl-1-propanol (AMP)* (99%, Thermo Scientific), *dimethyl sulfoxide (DMSO)* (99.8% Acros Originals), *monoethanolamine (MEA)* (99%, EMD Millipore Corporation), *acetonitrile* (100% VWR Originals), *sulfamic acid* (99%, Sigmaaldrich) and *sulfuric acid* (98%, VWR Chemicals). As previously mentioned, AMP and DMSO were the analytes of interest and acetonitrile, sulfamic acid and sulfuric acids were evaluated as solvents. Pure acetonitrile was used, whilst the acids were diluted with deionized water. Sulfamic acid was diluted to 0.1 M and sulfuric acid was diluted to 5 mM. MEA was investigated as an internal standard since it has a similar chemical structure to AMP. Additionally, it is relatively inexpensive and was readily available. Table 1 lists the chemicals used in this thesis.

Table 1. List of the chemicals used in this thesis, including their chemical structures.

Analytes	AMP	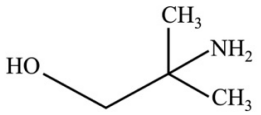
	DMSO	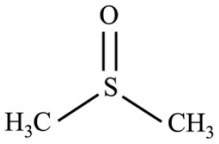
Solvents	Acetonitrile	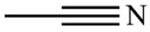
	Sulfamic acid	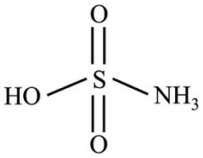
	Sulfuric acid	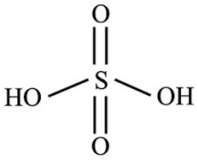
Internal standard	MEA	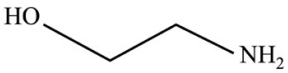

A 7890B Gas Chromatograph system from Agilent Technologies was used for all analyses in this thesis. The system was equipped with an autoinjector and an FID detector. Hydrogen was used as feed gas for the detector. Nitrogen was used as both makeup gas and carrier gas. Two columns were used throughout the period that the analyses were carried out, one HP-5 (30 m length, 0.320 mm diameter (widebore), 0.25 µm film thickness, 60°C to 325°C temperature limit) and one HP-5MS UI (30 m length, 0.320 mm diameter (narrowbore), 0.25 µm film thickness, 60°C to 325°C temperature limit), both from Agilent Technologies. The temperature and pressure programs were developed using trial and error and the final settings for the created methods, used to analyze the samples from the pilot plant, are summarized in Appendix A and B. The lab-created standard samples were prepared by mixing the different chemicals using magnetic stirrers and magnetic stirrer plates.

Additional equipment used to prepare the samples included plastic pipettes from VWR, GC vials from VWR and in some instances filters from LLG Labware. Since AMP is solid in room temperature, an oven set at 50°C was used to melt it. Two scales were used to measure the mass, one from VWR with two decimal precision, to measure the mass of the stock solutions and one from Fisher scientific (model: PA2214C) with four decimal precision, to measure the mass of the samples in the vials. The number of significant digits of the result values were based on the lowest number of significant digits in the calculations.

3.2 Qualitative analysis

The qualitative analysis was performed based on the principle described in Section 2.4.1. Three samples were prepared for each solvent. One containing AMP and the solvent, one with DMSO and the solvent and one with both the analytes in the solvent. The samples were then analyzed in the GC and the three generated chromatograms for each solvent were compared to investigate if the analytes could be identified. A match in retention times for both analytes would indicate that GC would be a suitable analysis method when using that solvent. Table 2 lists the prepared samples and their compositions.

Table 2. Lists the samples prepared for the qualitative analysis and their AMP and DMSO concentrations in wt%. (0.1 M sulfamic acid in water and 5 mM sulfuric acid in water).

	wt% AMP	**wt% DMSO**
AMP + Acetonitrile	0.3281	0
DMSO + Acetonitrile	0	0.2862
AMP + DMSO + Acetonitrile	0.3266	0.3266
AMP + Sulfamic acid	0.2690	0
DMSO + Sulfamic acid	0	0.4700
AMP + DMSO + Sulfamic acid	0.4629	0.3561
AMP + Sulfuric acid	2.755	0
DMSO + Sulfuric acid	0	3.968
AMP + DMSO + Sulfuric acid	3.964	3.344

Before the qualitative analysis could be performed, suitable GC method settings needed to be found for each solvent. These settings were developed through trial and error and were initially based on the settings used in a project conducted at Lund University, where a method was created for GC analysis of AMP and NMP (n-methyl-2-pyrrolidon) with ethanol as solvent[27]. Which settings that were changed, if a chromatogram did not provide baseline separation or gave poor peak shapes, were determined based om the appearance of the chromatograms. If the peaks were too small or showed fronting or tailing behavior, the split ratio was usually changed. A lower split ratio could for example result in bigger peak areas and a higher split ratio could result in less peak fronting or tailing (see Section 2.5.3, 2.6.4 and 2.6.5). If the resolution between the peaks was too low, the temperature program was usually investigated instead. Initial temperature, initial temperature hold time and the temperature ramp rate were common parameters that were changed to give better chromatograms. Introducing a hold time or lowering the ramp rate could for example contribute to a higher resolution (see Section 2.5.5). The settings that gave the best results for each solvent were then used in the qualitative analysis.

3.3 Quantitative analysis

The quantitative analysis methods used in this thesis included the external standard method and the internal standard method, of which the principles of these are described in Section 2.4.2. How these methods were investigated as possible methods for analyzing the mixtures of chemicals tested in this thesis is described in the following sections (Section 3.3.1 – 3.3.2). Both the external and internal standard methods include the creation of calibration curves, where a linear response would indicate that the curves are suitable for quantitative analysis. In this thesis, the linearity of the calibration curves was validated as described in Section 3.5. The selection of solvent and GC method settings was determined based on the results from the qualitative analysis, as explained in Section 4.1. The qualitative analysis showed that acetonitrile worked best as the solvent and the GC method settings used are given in Appendix A, Table A.1.

3.3.1 External Standard Method

Three dilution series were prepared to investigate the potential of the external standard method as a quantitative analysis method for AMP and DMSO solved in acetonitrile. One with AMP solved in acetonitrile, one with DMSO solved in acetonitrile and one with both AMP and DMSO solved in acetonitrile. Hence, three stock solutions were prepared with these combinations. The standard samples, used for creating a nine-point calibration curve for each combination, were then prepared from the stock solutions and gradually diluted with acetonitrile. The calibration series are given in Table 3.

Table 3. Displays the concentrations, in wt%, of the stocks and calibration series. AA is AMP solved in acetonitrile, AD is DMSO solved in acetonitrile and AAD is AMP and DMSO solved in acetonitrile.

	wt% AMP		wt% DMSO		wt% AMP	wt% DMSO
Stock (AA)	3.152	**Stock (AD)**	3.651	**Stock (AAD)**	4.589	4.749
1AA	3.152	**1AD**	3.651	**1AAD**	4.589	4.749
2AA	2.555	**2AD**	2.979	**2AAD**	3.775	3.907
3AA	2.428	**3AD**	2.813	**3AAD**	3.288	3.403
4AA	2.052	**4AD**	2.434	**4AAD**	2.937	3.039
5AA	0.4261	**5AD**	0.3925	**5AAD**	0.3829	0.4255
6AA	0.3209	**6AD**	0.3244	**6AAD**	0.3053	0.3392
7AA	0.2461	**7AD**	0.2624	**7AAD**	0.2260	0.2511
8AA	0.1710	**8AD**	0.1657	**8AAD**	0.1588	0.1765
9AA	0.07899	**9AD**	0.09247	**9AAD**	0.09762	0.1085

The reason for preparing these three dilution series was to investigate whether the calibration curves would be affected in the case that only one of the analytes would be present, compared

to when both would be present in the same mixture. This was done by comparing the linear regressions of the curves.

The standard samples in Table 3 were then analyzed three times each in sequences in the GC. The average GC area of each calibration standard was then plotted against their concentrations, resulting in three calibration curves that could be compared. An outlier test was also performed to investigate how much outliers affect a linear regression. The outliers were found using residual plots. These were then removed and replaced with a new value generated from a new GC analysis of that standard sample. The new linear regressions could then be compared to the previous linear regressions.

3.3.2 Internal Standard Method

The first step when testing the internal standard method as a possible analysis method, was to investigate the suitability of MEA as an internal standard. The second step was to create internal standard calibration curves and validate the linearity. For this, a stock solution containing AMP, DMSO and MEA solved in acetonitrile was prepared with a one-to-one ratio of wt% AMP/MEA and wt% DMSO/MEA (AADM). Then another stock solution with MEA diluted with acetonitrile, with a dilution factor of around 99, was prepared (AM). The two stock solutions and their compositions are listed in Table 4 below.

Table 4. Lists the two stock solutions AADM and AM, with their concentrations in wt%. The remaining composition of the stocks is the solvent acetonitrile. (AADM: Acetonitrile, AMP, DMSO, MEA. AM: Acetonitrile, MEA).

	wt% AMP	**wt% DMSO**	**wt% MEA**		**wt% MEA**
Stock (AADM)	1.886	1.886	1.886	**Stock (AM)**	1.010

A small portion of these two stocks were first analyzed separately in the GC and the generated chromatograms were compared. The AM stock was then added with an increasing amount in five different vials filled with the AADM stock, generating five standards with decreasing concentration ratios for AMP/MEA and DMSO/MEA. These standards were then used for calibration points for the internal standard calibration curve and their concentration ratios are summarized in Table 5.

Table 5. Shows the concentrations ratios of AMP/MEA and DMSO/MEA of the prepared standards for the internal standard calibration curve, with wt% as the concentration unit.

Acetonitrile/AMP/DMSO/MEA (AADM)	$\frac{\boldsymbol{AMP}\ [\boldsymbol{wt}\%]}{\boldsymbol{MEA}\ [\boldsymbol{wt}\%]}$	$\frac{\boldsymbol{DMSO}\ [\boldsymbol{wt}\%]}{\boldsymbol{MEA}\ [\boldsymbol{wt}\%]}$
1AADM	1.000	1.000
2AADM	0.8083	0.8083
3AADM	0.6089	0.6089
4AADM	0.3852	0.3852
5AADM	0.2944	0.2944

These standards were analyzed in the GC three times each and the areas of both analytes and internal standard were noted. The average area fraction of each standard sample was plotted against their concentration ratios to create the internal standard calibration curves. An outlier test was performed to investigate how much they affected the linear regressions of the curves.

3.4 Analysis of Samples from Pilot Plant

Parameters around GC analyses can change slightly over time and calibration curves should therefore be regularly updated to give the most representative results. This could be changes in temperature or pressure in the laboratory, changes in detector response or changes in column activity, among others. In this thesis, new calibration curves were produced when a new set of samples were taken at the pilot plant. In total, there were three sets of samples and hence three AMP and three DMSO calibration curves were constructed to analyze them. These calibration curves are presented in Appendix C, D and E. Samples from the pilot plant had to be regularly taken and analyzed throughout its operating time at VEAB. Therefore, in this thesis, they were exclusively analyzed with the external standard method, since it was the method first developed and evaluated. Acetonitrile was used as the solvent for all samples and calibration curves were prepared based on the principles explained in Section 2.4.2. In the external standard method tests in this thesis, the highest concentrations investigated were about 5 wt% of each analyte and therefore the samples were diluted to get within this range, based on their expected concentrations, as in Table 6. The dilution series and the samples were all analyzed with GC three times each in sequences. The average GC area of each calibration standard was then plotted against their concentrations, resulting in the calibration curves in Appendix C, D and E, Figure C.1, D.1 and E.1. The average GC areas of the standards, the linear regressions of the calibration curves and the dilution factors were then used to calculate the concentrations in the samples, according to Equation 8 below.

$$x = \frac{(y - m)}{k} DF \tag{8}$$

Where x is the unknown concentration of the sample, y is the average GC area, k is the slope of the calibration curve, m is the curves intercept with the y-axis and DF is the dilution factor.

Different types of samples were continually taken from the pilot plant throughout its time operating at VEAB. Liquid samples were taken at the lean solvent stream, before and after the heat exchanger, as well as at the gas outlet stream from the absorption column, see Figure 26. The flue gas samples were taken at the gas outlet stream from the pilot, as indicated in Figure 26. Since this was the first time the pilot plant was in operation on an industrial site, its performance was studied but the CO_2 captured was not removed or stored. Instead, the captured CO_2 was mixed with the gas stream out of the absorption column and lead back to the stack.

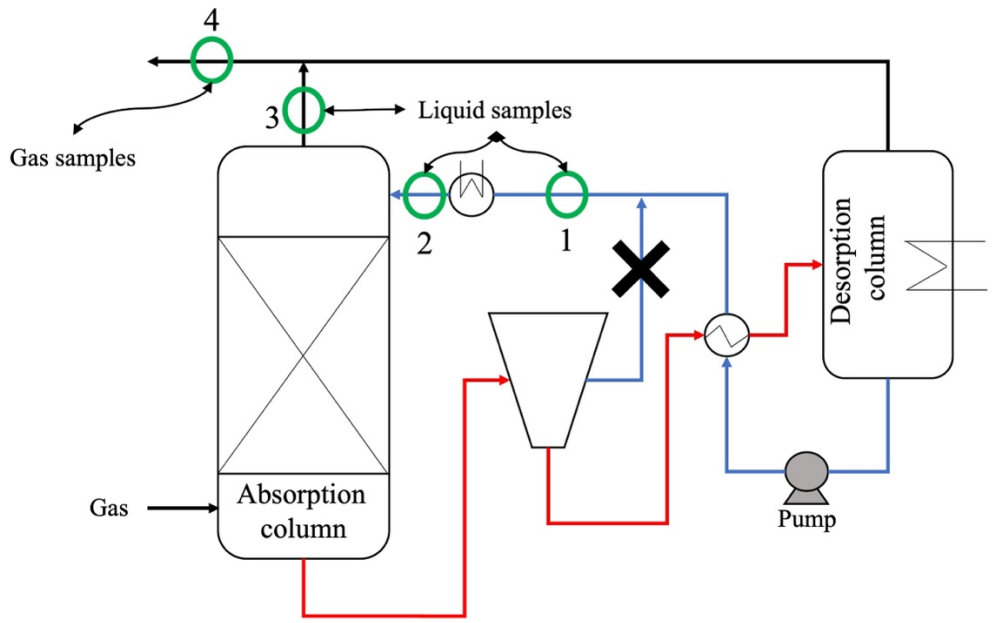

Figure 26. Shows where the different types of samples were taken in the pilot plant process flow sheet. The four spots are indicated with green circles and are marked 1 to 4. It should be noted that the separation unit was not active during the time the pilot was operating at VEAB and the lean-solvent stream out from the separator was hence not used.

Liquid samples were taken from installed valves on the pipes at spots 1,2 and 3 in Figure 26. The samples taken from spot 3 were also taken from a valve, although it is a gas stream. Here condensed gas was collected which allowed for a liquidized sample to be taken. The gas samples taken at spot 4 were taken with the method described in Section 2.3.

In total six different liquid samples were analyzed throughout the operating time of the plant at VEAB. The first one (sample L1) was taken on March 9 from spot 1. At this point, the mechanics of the pilot were tested to investigate how well it could transport the absorption mixture. No gas stream was therefore introduced at this point and the sample was expected to contain an AMP/DMSO ratio of about 1 to 3, since this was the volume ratio of the absorption mixture. Three other liquid samples were taken on March 28, April 11 and April 12 respectively (sample L2, L3 and L4), from spot 1. At this point, a gas stream from the industrial site had been introduced and these samples were hence expected to have concentrations below the initial concentrations of the absorption mixture. Sample L3 and L4 were taken at different times while emptying the stripper tank. L3 at the start, which made the sample representable of the bottom part of the tank and L4 when half of the tank had been emptied, which made the sample representable of the middle part of the tank. Samples L2, L3 and L4 all contained some precipitate and only the liquid phase was analyzed with GC. On March 28 another sample was taken from spot 3. The concentrations of this sample were less predictable and hence diluted with three different dilution factors (sample L5a, L5b and L5c). Additionally, a sample from the AMP feed stock used in the pilot (L6), which could consist of up to 10 vol% impurities. The dilutions of the liquid samples are summarized in Table 6.

Two samples were also taken on March 14. These were solid samples (samples S1 and S2) and resulted from a clogging in the lean solvent stream, which caused some solution to leak out from the pipe and precipitate on its outside, as well as on the inside. S1 was taken from the

inside of the pipe and S2 was taken from the leaked precipitation on the outside of the pipe. They were not taken from the tap at spot 1, but in close connection to it. The solid samples are also listed in Table 6.

Two gas samples were taken from spot 4 on April 4 (samples G1 and G2). These were taken using the cartridge method sampling technique, described in Section 2.3. They were first sent to a certified lab, which extracted the thermosorb with acetonitrile, before they were analyzed in this thesis research and therefore no dilution or other pretreatment was needed for these samples. There was hence no need to measure the mass of the samples and that is why it is not included in Table 6, where the gas samples are listed. Sample G1 was extracted two times at the certified lab, resulting in two samples, samples G1_1 and G1_2. The amount of analyte found in G1_1 and G1_2 would hence need to be added together to represent the amount of sample G1. More detailed information about how the certified lab pretreated these samples is presented in Appendix E.

Table 6. Lists all samples analyzed from the pilot plant throughout its time operating at VEAB, the spring 2023. Liquid, gas and solid samples are listed. The table includes the amount of sample analyzed, the amount of the solvent acetonitrile, the dilution factor, the sampling spot in Figure 26, the sampling date at the pilot and which calibration curves that were used for the analyses can be found in Appendix C-E.

		Sample [g]	Aceto-nitrile [g]	DF	Sampling spot	Sampling date	Calibration curves (Figure)	GC settings (Table)
Liquid samples	**L1**	0.99	21.24	22	1	9/3-23	C.1	A.1
	L2	0.9191	20.0523	22.82	1	28/3-23	C.1	A.1
	L3	1.01	20.02	20.8	1	11/4-23	D.1	A.1
	L4	1.00	20.00	21.0	1	12/4-23	D.1	A.1
	L5a	1.01	20.03	20.8	3	28/3-23	D.1	A.1
	L5b	1.00	9.00	10.0	3	28/3-23	D.1	A.1
	L5c	1.00	4.00	5.00	3	28/3-23	D.1	A.1
	L6	1.01	20.04	20.8	AMP stock	28/3-23	D.1	A.1
Gas samples	**G1_1**	-	-	-	4	4/4-23	E.1	A.2
	G1_2	-	-	-	4	4/4-23	E.1	A.2
	G2	-	-	-	4	4/4-23	E.1	A.2
Solid samples	**S1**	0.0634	18.0421	286	Pipe inside	14/3-23	C.1	A.1
	S2	0.0552	17.489	318	Pipe outside	14/3-23	C.1	A.1

3.5 Method validation

Method validation is the process of examining the suitability of an analytical method for its intended purpose. How this is done and what the requirements are depends on what the method is to be used for and the field in which it is going to operate. In some cases, an indication of the composition of the sample can be enough, whereas in other cases a more detailed description is required.[16] In this thesis, an indication of the concentrations was set as a requirement and the method was validated based on selectivity, linearity and precision.

3.5.1 Selectivity

The selectivity of an analytical method is defined as the extent to which the method can determine particular analytes without interference from other components in the sample.[16] In chromatographic analyses, a reasonable selectivity requirement is that there is baseline separation between the peaks of interest. In this study, the selectivity was measured using the following version of Equation 3 for calculating the resolution, R_s.

$$R_s = \frac{0.589\Delta t_R}{w_{1/2av}} \tag{9}$$

Where again, $w_{1/2av}$ is the average of the peak width at half their peak heights and Δt_R is the difference in retention time between the two peaks. As explained in Section 2.4, a resolution of above 1.5 is highly desirable for quantitative analysis[16] and therefore this was set as the selectivity requirement for all chromatograms in this thesis.

3.5.2 Linearity

Linearity is a measurement of linear behavior from a calibration curve. A curve that follows a straight line shows that the response is proportional to the amount of analyte and that it is capable of being used for quantitative analysis.[16] In this thesis, between 5 and 10 calibration points with varying concentrations were used for each calibration curve and each sample was analyzed three times. The average response of each calibration point was plotted against their respective concentrations and the calibration curves were constructed with the least square method. The least square method draws a straight line that best fits with the points. The first aspect of assessing the linearity of the calibration curves was a visual evaluation of the scatter of data points. In the ideal case, the scatters are close to the calibration curve and show random behavior, in which some are above, and some are below the line. A visual systematic scatter could be an indication of nonlinearity.[16] Residual plots were used to help with this visualization. A residual is the difference between the observed value and the value predicted by the mathematical model and is calculated according to Equation 10.

$$d_i = y_i - y \tag{10}$$

Where d_i is the residual, y_i is the measured value, y is the value predicted by the mathematical model. The residual plot helps with indicating outliers and curvatures among the data points.[16]

The square of the correlation coefficients, R^2, was also calculated for all calibration curves. This value is the fraction of the variation in the y-variable explained by the x-variable and can be

used to indicate linearity. The value ranges from 0 to 1, where the closer the value is to 1, the better the linear approximation.[16] R^2 was calculated using Equation 11.

$$R^2 = \frac{[\sum(x_i - \overline{x})(y_i - \overline{y})]^2}{\sum(x_i - \overline{x})^2 \sum(y_i - \overline{y})^2} \tag{11}$$

Where $\overline{x}$ is the average of all x-values and $\overline{y}$ is the average of all the y-values.[16]

The intercept with the y-axis for the linear regression of the calibration curve (the m-value) also gives an indication of the linearity. Since a blank sample ideally would result in zero response, the m-value should have a value that is close to zero.[16] In this study the R^2-values and m-values of all linear regressions of the calibration curves were calculated using built in functions in Microsoft Excel which uses Equation 11 to calculate the R^2-values.

3.5.3 Precision

The precision of a method is a measurement of the agreement among individual test results for repeatable implementations of the method. It is usually displayed as a standard deviation, a standard uncertainty or a confidence interval.[16] In this thesis, the standard deviation was used to measure precision. This was done by analyzing every calibration point and sample three times and calculating the standard deviation of the resulting concentration corresponding to the points. The standard deviation, *s*, was calculated using Equation 12.

$$s = \sqrt{\frac{\sum(x_i - \overline{x})^2}{n - 1}} \tag{12}$$

Where x_i is the value of the i:th data point, $\overline{x}$ is the mean value of the data set, n is the number of data points.

4 Results and Discussion

In this section, the results from the qualitative and quantitative analyses as well as the analyses of the samples taken at the pilot plant are presented and discussed.

4.1 Qualitative analysis

The results from the qualitative analysis showed that acetonitrile worked well as a solvent whilst aqueous sulfamic acid and sulfuric acid did not work as well. How this was concluded is described in the following sections (Section 4.1.1 - 4.1.3) where the results for each solvent are presented individually.

4.1.1 Acetonitrile as solvent

The chromatograms from the GC analysis of the three samples with acetonitrile as solvent, in Table 2 (Section 3.2), are presented in Figure 27 below. The GC method settings used for the analysis was found by trial and error and can be found in Appendix A, Table A.1.

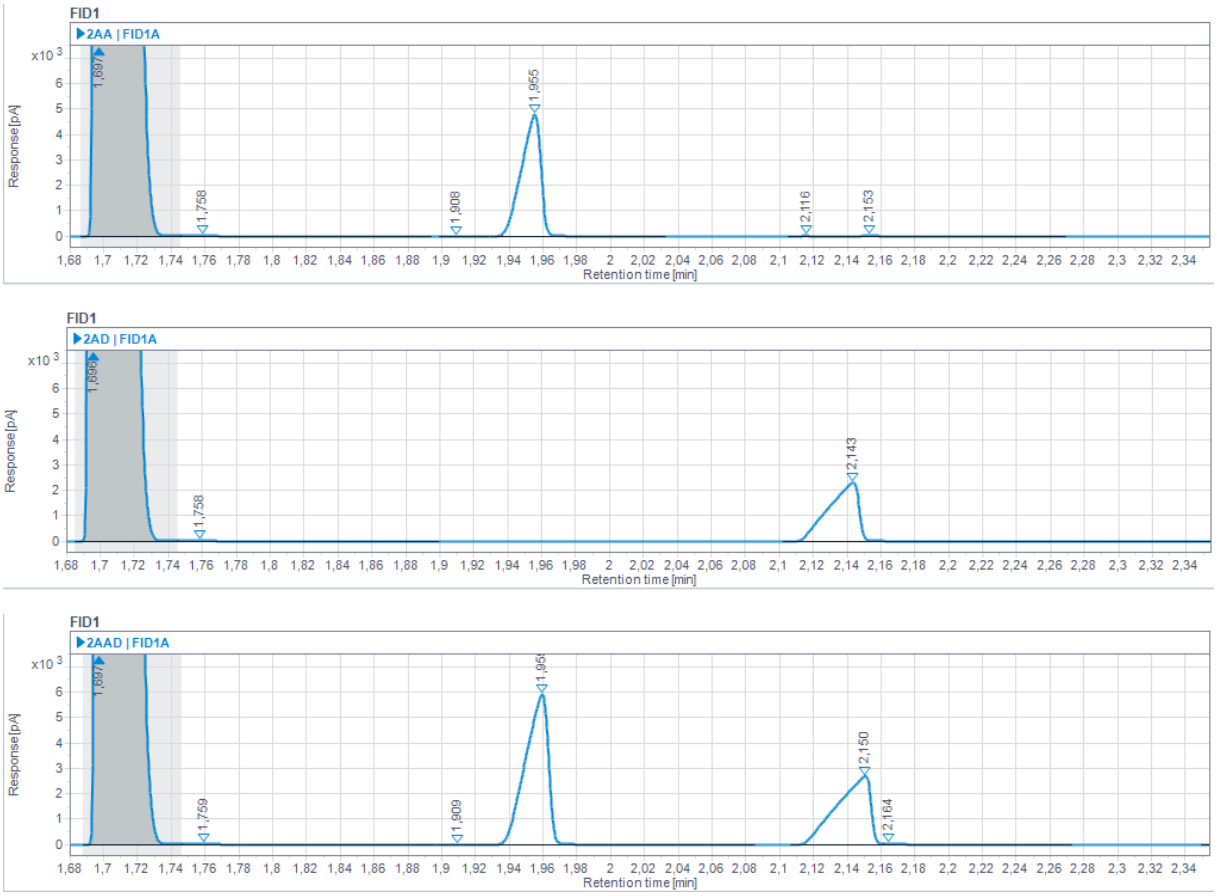

Figure 27. Shows chromatograms from GC analysis of the samples with acetonitrile as solvent in Table 2. The chromatogram at the top contains AMP and acetonitrile, the chromatogram in the middle contains DMSO and acetonitrile and the chromatogram at the bottom contains AMP, DMSO and acetonitrile. The large peak highlighted in gray at the left of all chromatograms is acetonitrile. The elution follows the order of acetonitrile, AMP and lastly DMSO.

The chromatograms in Figure 27 show significant peaks for AMP and DMSO as well as for acetonitrile. Additional peaks can be noticed but with insignificantly small peaks sizes. The

chromatogram at the top was generated from the sample containing AMP solved in acetonitrile and the chromatogram in the middle contains DMSO solved in acetonitrile. The chromatogram in the bottom contains both analytes and a comparison of the retention times between the chromatograms shows that they match for each peak. This suggests that both AMP and DMSO can be identified in mixtures where both are present. That AMP elutes before DMSO was expected since AMP has a lower boiling point than DMSO (165°C[10] compared to 189°C[28]). The separation between the AMP and DMSO peaks also showed to be sufficient with a resolution of 8.2, which is above the minimum value of 1.5, and was calculated from Equation 9 with the measured parameters in Table 7.

Table 7. Lists the width at half peak height and retention times for AMP and DMSO and the resolution between them. The resolution was calculated using Equation 9.

	$w_{1/2}$	t_R	R_s
AMP	0.015	1.959	8.2
DMSO	0.023	2.150	

The peaks in Figure 27 show a slight peak fronting behavior, especially the DMSO peaks. This could be due to the relatively large peak areas, which could indicate that the concentrations in the samples might be too high for this method. However, it should be noted that the visual representation of chromatographic peaks can be greatly influenced by the scale of the x- and y-axes. Based on the large number of observations throughout this thesis, it could be noted that, in general, DMSO peaks consistently showed a greater degree of peak fronting behavior compared to AMP, even at lower concentrations. This influences the retention times slightly, where smaller peaks get an earlier retention time, but not to the extent to which the peaks cannot be identified.

These results suggest that AMP and DMSO can successfully be qualitatively analyzed with GC when using acetonitrile as the solvent.

4.1.2 Sulfamic acid as solvent

The chromatograms from the GC analysis of the three samples with sulfamic acid as solvent, in Table 2 (Section 3.2), are presented in Figure 28 below. The GC method settings used for this analysis were found by trial and error and are presented in Appendix B, Table B.1.

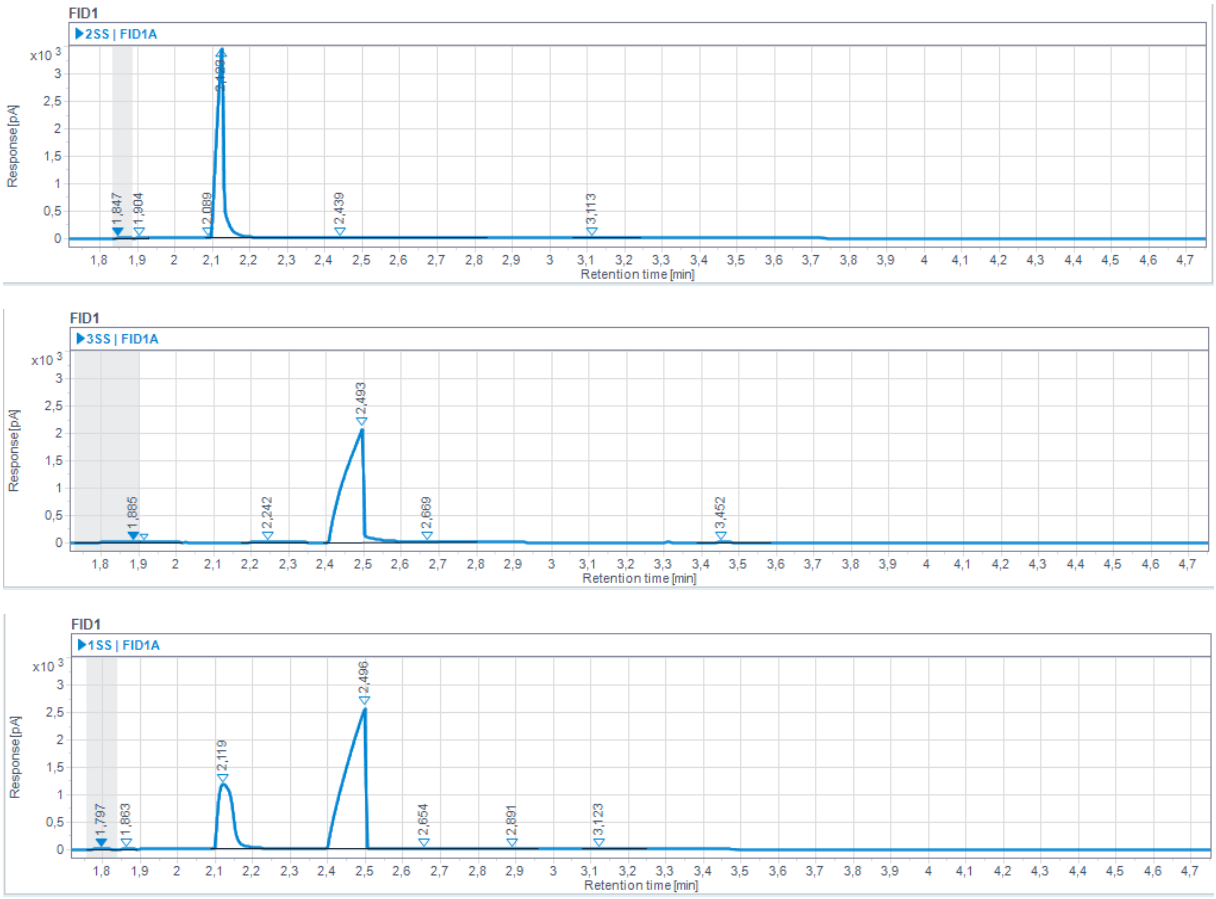

Figure 28. Shows chromatograms from GC analysis of the samples with sulfamic acid as solvent in Table 2 (Section 3.2). The chromatogram at the top contains AMP and sulfamic acid, the chromatogram in the middle contains DMSO and sulfamic acid and the chromatogram at the bottom contains AMP, DMSO and sulfamic acid.

The chromatograms in Figure 28 show significant peaks for AMP and DMSO. It should be noted that 0.1 M sulfamic acid in water should not be detectable by the FID detector since it is an inorganic solvent and no peak for the solvent is hence given. The peak shapes are not as ideal as when acetonitrile was used as the solvent. The AMP peak in the chromatogram at the top shows slight peak tailing behavior and when both AMP and DMSO are present, the AMP peak gives a slightly rounded top. The DMSO peaks once again show some peak fronting behavior. A comparison of the retention times between the chromatograms does however indicate that it might be possible to identify both AMP and DMSO in mixtures where both are present with sulfamic acid as solvent. The separation also seems to be sufficient with a resolution of 4.3 (4.3 > 1.5), which was calculated from the measured parameters in Table 8.

Table 8. Lists the width at half peak height and retention times for AMP and DMSO and the resolution between them. The resolution was calculated using Equation 9.

	$w_{1/2}$	t_R	R_s
AMP	0.043	2.119	4.3
DMSO	0.060	2.496	

These results indicate that sulfamic acid possibly could be used as solvent for qualitative GC analysis of AMP and DMSO. However, later tests suggest otherwise. Figure 29 shows multiple chromatograms from a sequence that was meant to be used for the quantitative analysis. The image displays a comparison of three chromatograms from the same sample ran three times.

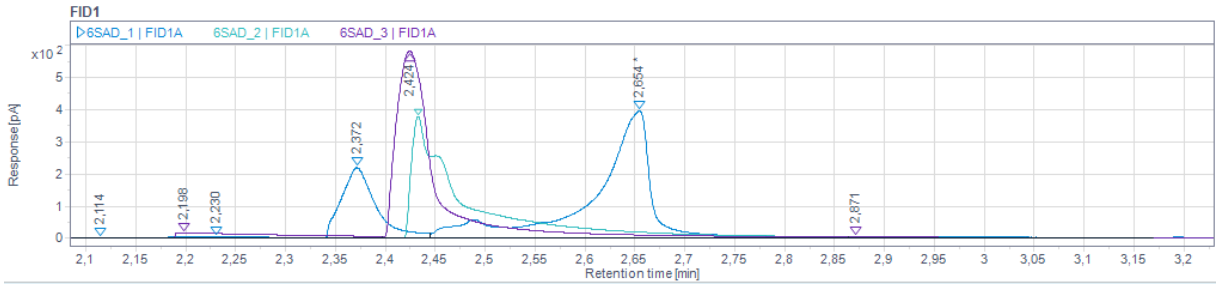

Figure 29. Shows three chromatograms from the same sample ran three times. The sample contains both AMP and DMSO. In an ideal situation these chromatograms would be next to identical, since it is the same sample, which is not the case here.

Since the image in Figure 29 shows a comparison of three runs of the same sample, the chromatograms should ideally be next to identical, with one peak for AMP and one for DMSO. However, it can be seen that the peak shapes and retention times vary to a large extent. The reason for this could be due to the large amount of water present in the solvent and this is further discussed in the next section, Section 4.1.3. The chromatograms in Figure 29 suggests that 0.1 M sulfamic acid in water might not be a suitable solvent for GC analysis of AMP and DMSO after all.

4.1.3 Sulfuric acid as solvent

The chromatograms from the GC analysis of the three samples with sulfuric acid as solvent, in Table 2 (Section 3.2), are presented in Figure 30. The GC method settings used for this analysis was found by trial and error and can be found in Appendix A, Table A.1.

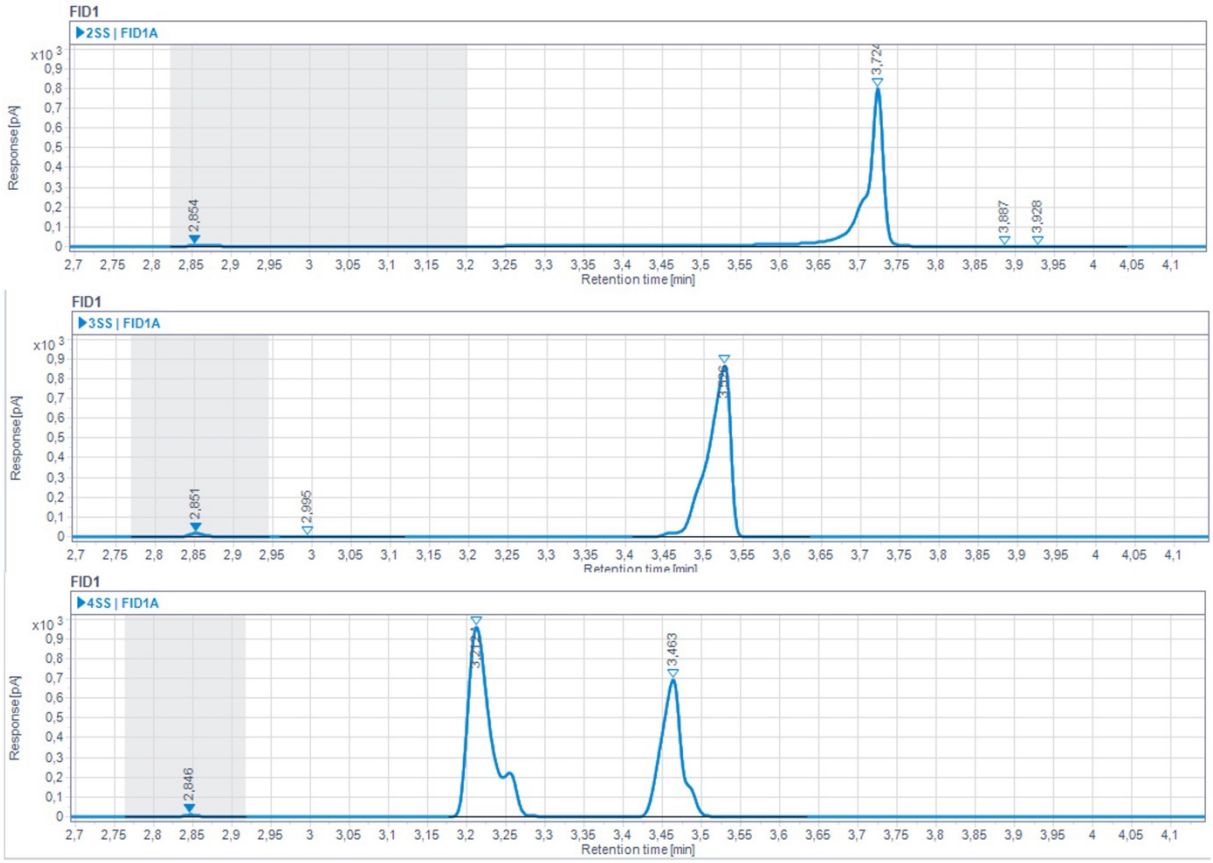

Figure 30. Shows chromatograms from GC analysis of the samples in Table 2 with sulfuric acid as solvent. The chromatogram at the top contains AMP and sulfuric acid, the chromatogram in the middle contains DMSO and sulfuric acid and the chromatogram at the bottom contains AMP, DMSO and sulfuric acid.

The chromatograms in Figure 30 show significant peaks, but the shapes are of varying quality with some fronting and others tailing. The first peak in the sample with both AMP and DMSO also gives a split peak, which is not ideal. Additionally, these peaks cannot be identified by comparing the chromatograms since the retention times do not match. The peak in the sample with only DMSO and sulfuric acid also elutes earlier than the peak from the sample with only AMP and sulfuric acid, which was unexpected and not observed for the other solvents tested in this thesis. Theoretically, AMP should elute earlier because it has a lower boiling point than DMSO. The separation of the peaks in the sample with both analytes was however sufficient, with a resolution of 5.4 (5.4 > 1.5) and was calculated with the retention times and half-height peak width in Table 9.

Table 9. Lists the width at half peak height and retention times for the two peaks and the resolution between them. The resolution was calculated using Equation 9.

	$w_{1/2}$	t_R	R_s
Peak 1	0.028	3.212	5.4
Peak 2	0.027	3.463	

Significant peaks and sufficient separation indicate a potential for sulfuric acid as a solvent, but the variation in retention times makes it unusable for qualitative GC analysis of AMP and DMSO.

The reason why both sulfamic acid and sulfuric acid did not work well as a solvent could be because both solvents contain large amounts of water, which was not the case for acetonitrile. Water is a common solvent in GC analyses, but it has been reported as not being well suited for all GC applications. Water has a large expansion volume compared to other solvents, which can generate fluctuations in retention times between different analyses of the same sample. Too much water in the detector can also extinguish the flame, which can give significant variations in peak size.[29] This could explain why some chromatograms in this thesis gave promising result while some did not. Water is also a polar solvent and since non-polar columns were used, this could also have influenced the varying results.

4.2 Quantitative analysis

Since acetonitrile proved to be the most successful solvent for the qualitative analysis, the quantitative analysis was performed with acetonitrile as the solvent. The GC method settings used for all tests in this section can be found in Appendix A, Table A.1.

The quantitative analysis showed promising results for both the external and the internal standard method. Some indications that the slope of the external calibration curves for AMP was slightly affected by the presence of DMSO in the mixture were also given from the results. Additionally, the outlier test indicated that outliers did not affect the linearity of the external calibration curves significantly. How these results were concluded is described in the following sections (Section 4.21 – 4.2.2).

4.2.1 External Standard Method

The calibration curves generated from the GC analysis of the samples in Table 3 (Section 3.3.1) are displayed in Figure 31, along with their respective residual plots.

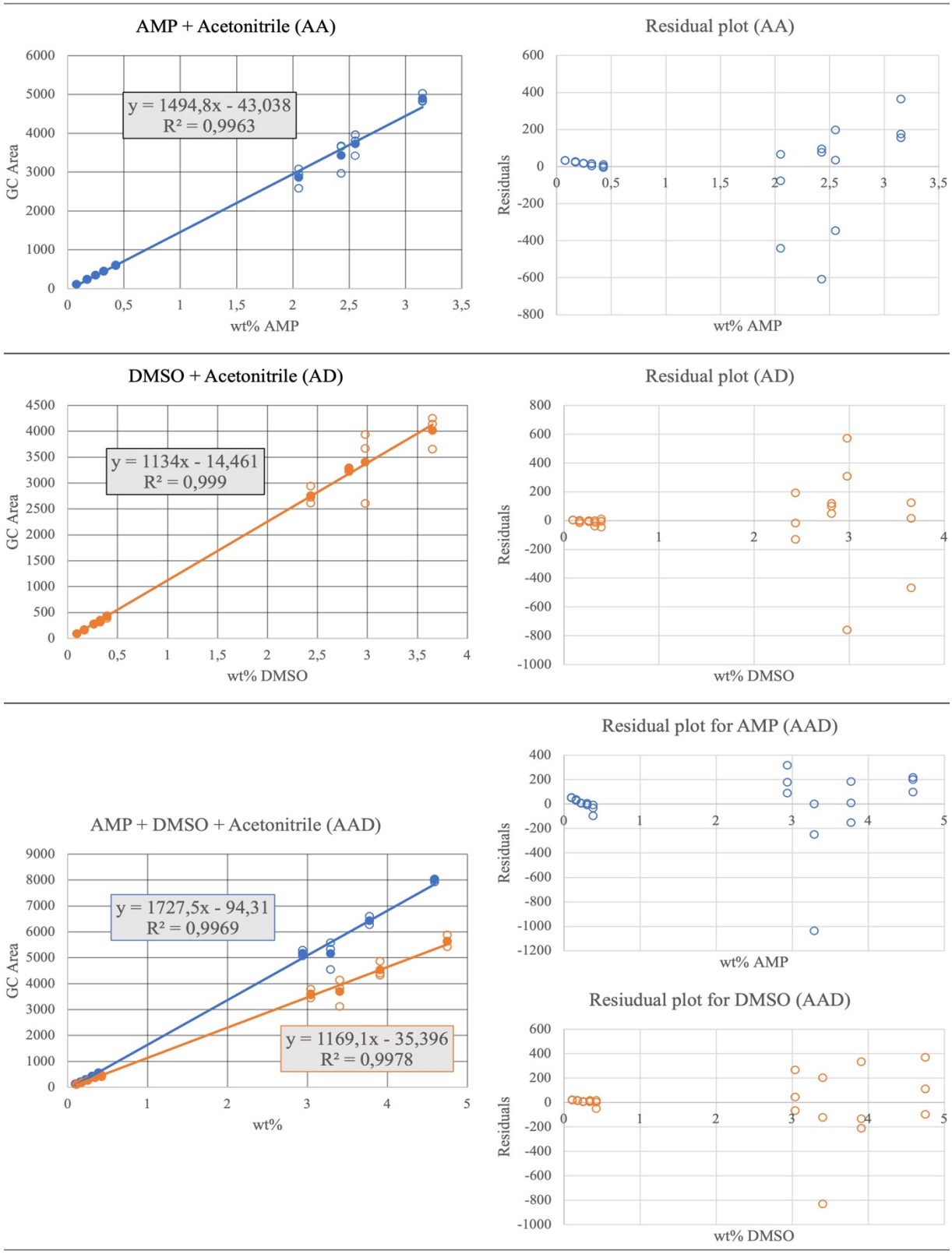

Figure 31. The column to the left shows the calibration curves from the GC analysis of the prepared samples in Table 3 (Section 3.3..1). Their respective residual plots are displayed in the column to the right. Curves and points in blue represent AMP and orange represent DMSO. For each concentration point (x-value) in the calibration curves, four values are shown. Three of them are unfilled circles which are the measured GC area from the three runs. One is a filled in circle which is the average of the measured values, from which curves are created from. The rectangles highlighted in grey is the linear regression for its respective curve.

The linear regressions give high R^2-values for all calibration curves in Figure 31 with values well over 0.99, which indicate a linear response. The residual plots for the two DMSO curves show that the measured responses are scattered with random behavior around the average derivation of 0, which also indicates that the responses are linear. Both the residual plots for the AMP curves shows a random distribution for the higher concentration points. The residuals for the lower concentrations might however show a slight tendency to tilt with a negative slope. This could be caused by a shift in linearity between the concentration ranges, or by random errors. If these curves would be used for concentration determination of actual samples with a precision requirement, this might be of interest to investigate further. However, since these deviations are relatively small over the small concentration ranges and that the R^2-values are high, the responses can be interpreted as linear enough for the purpose of this analysis.

The residual plots also reveal some outliers that deviate from the average deviations more than outer points. This is especially the case for the higher concentration ranges, particularly the third-highest concentration point in the AA curve, the second-to-highest concentration point in the AD curve and both the third-to-highest concentration points in the two AAD curves. This could indicate deviation from linearity at higher concentrations of the two analytes, or it could be caused by random errors. There are numerous factors in GC analyses that can cause random errors, like slight variations in detector response and injection volume (even when an autosampler is used). It should also be noted that the two points in the AAD curves originate from the same chromatogram and since the residuals seem to be randomly distributed, the outliers likely occur from random errors. These outliers might also influence the slight negative slope behavior for the low AMP concentration points. If these curves were to be used for a quantitative analysis of an actual sample with requirements of a certain precision, it might have been valid to replace the outliers with new measurement points. For the purpose of this thesis, the high R^2-values and the random scatter of residuals indicates that the detector response is relatively linear, and that the external standard method is a suitable method for quantitative analysis.

Table 10 summarizes the linear regressions of the curves in Figure 31.

Table 10. Lists the linear regressions of the calibration curves in Figure 31, including the slopes, interceptions with the y-axis and the R_2-values. (AA: AMP solved in acetonitrile. AD: DMSO solved in acetonitrile. AAD: AMP and DMSO solved in acetonitrile).

	AMP		**DMSO**	
	Linear Regression	R^2	Linear Regression	R^2
AA	$y = 1494.8\text{x} - 43.038$	0.9963	-	-
AD	-	-	$y = 1134.0\text{x} - 14.461$	0.9990
AAD	$y = 1727.5\text{x} - 94.310$	0.0069	$y = 1169.1 - 35.396$	0.9978

When comparing the linear regressions for the curves in Figure 31, it can be seen that the slopes of the DMSO curves got similar results with 1134.0 when DMSO was the only analyte (the AD mixture) and 1169.1 in the presence of AMP (the AAD mixture). In contrast, the slopes of the

AMP curves showed a larger difference of 1494.8 when AMP was the only analyte (the AA mixture) and 1727.5 when DMSO was present (the AAD mixture). This suggests that the presence of both analytes might influence the response to AMP slightly. This result is surprising and would not be expected under ideal circumstances. There are a few possible explanations for this result, including baseline disturbance introduced by DMSO or interactions between DMSO and the detector or carrier gas. This should however also have affected the DMSO response, which does not seem to be the case. Since the curves were constructed on different occasions, a likely explanation is instead that some change could have been introduced in the GC setup. The GC setup is sensitive to minor changes like temperature, pressure, column degradation, injection volume, liner impurities, carrier gas and detector feed gas flow rates, to mention a few. The difference in concentration range that the curves cover, in combination with a possible shift in linearity discussed earlier, could also have an influence. Additional tests would be necessary to investigate this. With these insights it was decided that the analyses of the samples from the pilot plant would be performed with standard samples that were prepared with as similar composition to the assumed composition in the sample as possible to mitigate this possible effect.

To investigate how much outliers would affect the result of a linear regression, an outlier test was performed on two calibration curves that were later used in this thesis to analyze samples from the pilot plant. The original curves with outliers and the new curves where the outliers were replaced by new GC results are displayed in Figure 32.

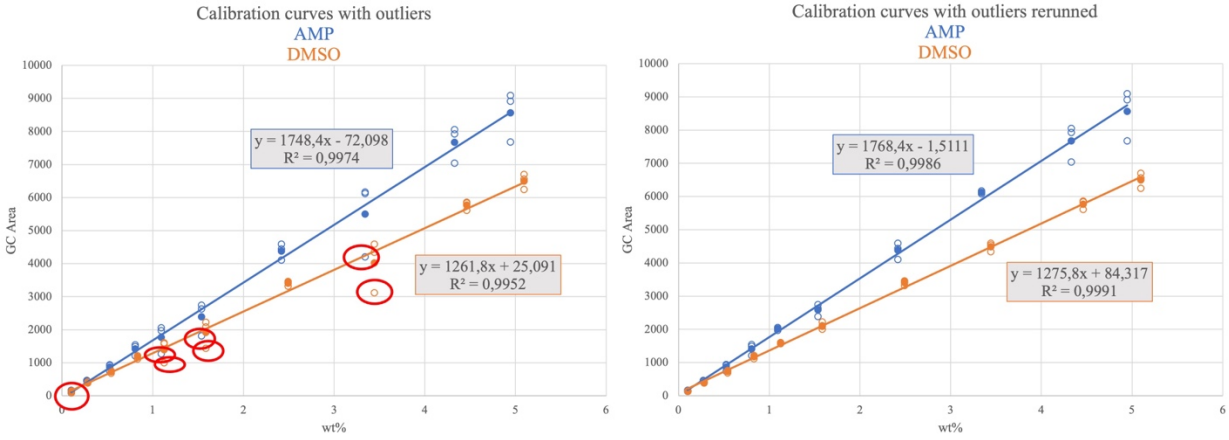

Figure 32. Shows external calibration curves used in this thesis to analyze samples from the pilot plant. The curves were created from a set of lab prepared samples that are listed in Appendix D. The two curves to the left are based on measurements that gave a few outliers, the points with red circles around them. The two curves to the right are based on the same measurements but here the outliers are replaced with new measurements from the GC for those points.

A comparison between the linear regressions, for the curves with some outliers and the curves with new values for those outliers, shows that the R^2-values increased for both the AMP and the DMSO curve. The R^2-value of the AMP curve went from 0.9974 to 0.9986 and the R^2-value of the DMSO curve from 0.9952 to a value of 0.9991. This suggests that the linearity increased which is expected since the residuals deviate less from the average deviation. However, the slopes of the curves do not seem to be largely influenced. The slope of the AMP curve goes from a value of 1748.4 to a value of 1769,4 and the slope of the DMSO curve goes from 1261.8 to 1275.8. These are relatively small changes and suggests that the few outliers get averaged

out and do not affect the linear regression significantly. It should also be noted that the outliers of the AMP curve and the DMSO, in Figure 32, arise from the same chromatograms. If an outlier resulted from an AMP peak in the chromatogram, the DMSO peak usually also resulted in an outlier for that chromatogram. This was a regular occurrence throughout the tests done in this thesis. That both peaks were affected in some chromatograms, when external calibration curves were created, suggests that an irregularity occurred due to random errors in the GC analysis.

The results provided in this section show that the detector response to AMP and DMSO solved in acetonitrile is linear and the external standard method is hence a suitable method for approximative quantitative analysis.

4.2.2 Internal Standard Method

Figure 33 shows the generated chromatograms from the GC analysis of stock solution AM and stock solution AADM reported in Table 4 (Section 3.3.2). The GC method settings used for these analyses are summarized in Appendix A, Table A.1.

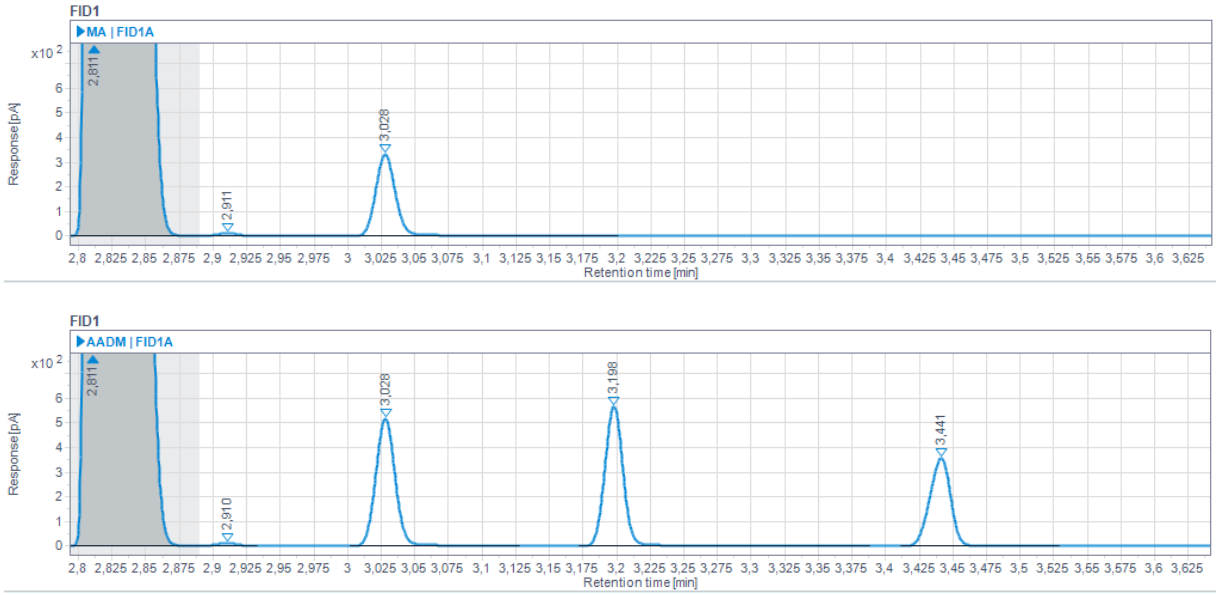

Figure 33. The chromatogram at the top is from the AM stock solution (MEA solved in acetonitrile). The chromatogram in the bottom is from the AADM stock solution with a one-to-one concentration ratio for AMP/MEA and DMSO/MEA (solved in acetonitrile).

The chromatogram in Figure 33 shows a good shape for all the peaks and sufficient separation, with resolutions above 1.5 for all peaks, see Table 11 below. MEA can also be identified by comparing the retention times between the chromatograms. This indicates that MEA could successfully be used as an internal standard for a mixture with this combination of chemicals.

Table 11. Lists the resolution calculated from the measured retention times, peak width at half height and Equation 9.

	$w_{1/2}$	t_R	R_s
MEA	0.016	3.028	6.7
AMP	0.014	3.198	9.2
DMSO	0.017	3.441	

Since MEA showed potential as an internal standard, the prepared standards in Table 5 were analyzed with GC, resulting in the calibration curves in Figure 34.

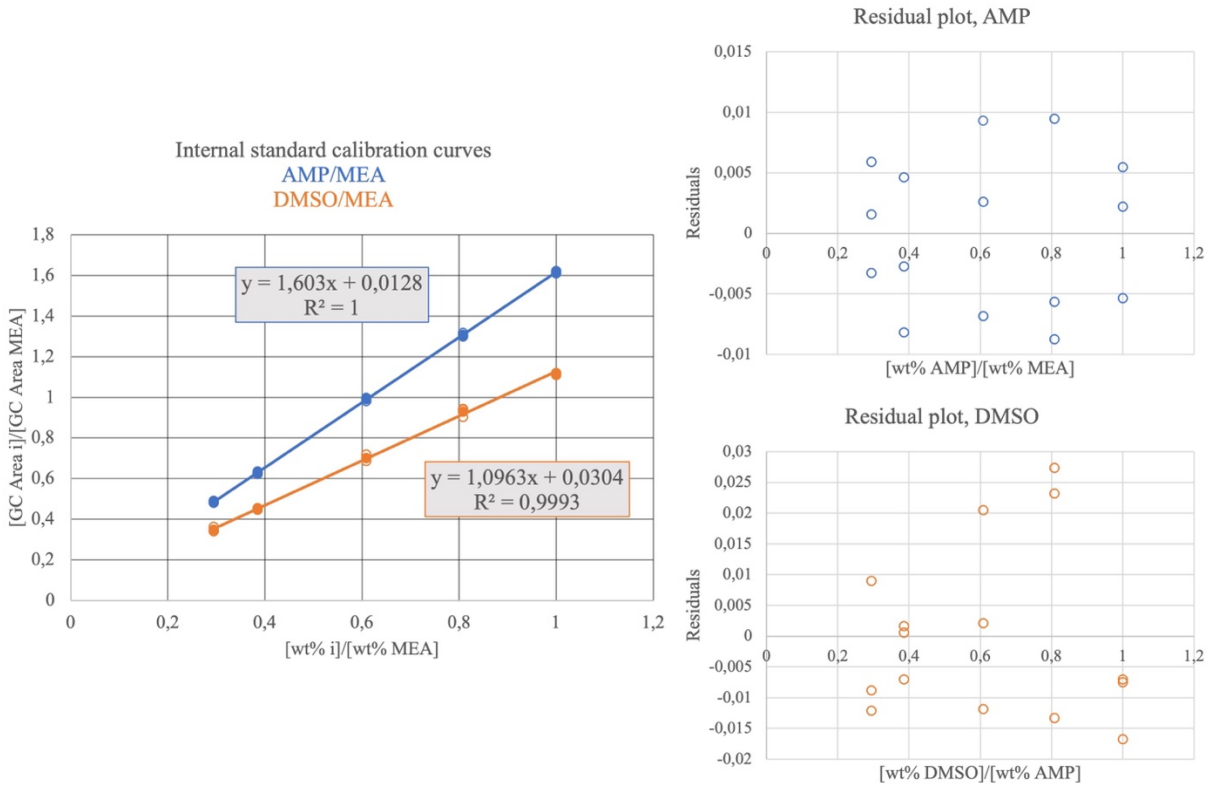

Figure 34. Internal standard calibration curves and their residual plots for the samples listed in Table 5 (Section 3.3.2). AMP is shown in blue and DMSO in orange. i denotes AMP or DMSO. For each concentration point (x-value) in the calibration curves, four values are shown. Three of them are unfilled circles which are the measured GC area from the three runs (difficult to identify due to how close they are to the average value). One is a filled in circle which is the average of the measured values, from which curves were created. The rectangles highlighted in grey are the linear regressions for the respective curve.

The linear regression for the calibration curves in Figure 34 gives a R^2-value of 1.000 for AMP/MEA and 0.9993 for DMSO/MEA. The residual plots display a random scatter around the average derivation with no clear outliers, with a tight span for all calibration points. The R^2-values and the residual plots strongly indicate a linear relationship. The response factors were determined as the slope from the linear regressions to 1.603 for AMP/MEA and 1.096 for DMSO/MEA. These results show that the internal standard method, with MEA as an internal standard, is a suitable quantitative GC analysis method for a mixture of these chemicals.

During the construction of the internal standard calibration curves in Figure 34, sample 2AADM and 3AADM gave slightly different peak shapes in one of the runs for all the peaks. These peaks had slightly more rounded tops than the peaks given in the other runs. This is likely due to random errors and these samples were therefore analyzed again to give new results. The new peaks gave more similar shapes to other runs and what one would expect. The ratios are summarized in Table 12.

Table 12. Compares the ratios of the original results and the new results when the samples were analyzed in the GC again, for sample 2AADM and 3AADM in Table 5.

	AMP/MEA	**DMSO/MEA**
2AADM		
Original ratios	1.303	0.9440
New ratios	1.303	0.8999
3AADM		
Original ratios	0.9915	0.7184
New ratios	0.9880	0.6961

In the external standard method, differences in peak shapes were either averaged out buy multiple runs or corrected with a new analysis for those samples. In the internal standard method however, these differences do not influence the results significantly since the error usually affects all peaks to similar degree and hence give minor changes to the ratios. This can be seen in Table 12 which shows that the difference of the ratios from different runs with different peak shapes is insignificant. This result is expected and shows the advantage of using this method. However, different compositions in a mixture can behave differently in GC analyses and these results suggest that the advantage of the internal standard method applies for the combination of AMP, DMSO, MEA and acetonitrile. Samples taken from the pilot plant would likely contain a variety of additional chemicals and possibly affect these ratios. Further experimental work would have to be conducted to investigate the potential of MEA as an internal standard for samples from the pilot plant.

4.3 Analysis of Samples from Pilot Plant

The concentrations of AMP and DMSO for the pilot plant samples in Table 6 (Section 3.4), resulting from GC analysis, are given in Table 13. The concentration calculations, together with the linear regressions of the external calibration curves, are given in Appendix C - E.

Table 13. Lists the concentrations of AMP and DMSO in each analyzed sample from the pilot plant, in wt%. The concentrations are calculated using Equation 8, the dilution factors in Table 6 and the results of the linear regressions from the GC analyses (the linear regression used for each sample is given in Appendix C – B). Standard deviation (STD) and percentage standard deviation (STD%) for each concentration is also included. The standard deviations are calculated using Equation 12.

		wt% AMP	STD	STD%	wt% DMSO	STD	STD%
Liquid samples	**L1**	20.76	1.105	5.322	64.28	1.454	2.262
	L2	11.04	0.1874	1.698	41.93	0.2367	0.5646
	L3	10.93	1.054	9.641	54.15	1.847	3.411
	L4	11.23	1.741	15.50	55.15	3.476	6.308
	L5a	-	-	-	-	-	-
	L5b	-	-	-	-	-	-
	L5c	-	-	-	0.4493	0.008971	1.997
	L6	100.0	5.521	5.519	-	-	-
Solid samples	**S1**	50.20	0.3731	0.7434	19.44	0.4730	2.433
	S2	57.43	0.4291	0.7472	19.31	0.6127	3.172
Gas samples	**G1_1**	-	-	-	0.3233	0.02273	0.07031
	G1_2	-	-	-	0.07147	0.002957	0.04138
	G2	-	-	-	-	-	-

The L1 sample was collected during an assessment of the ability of the pilot to transport the absorption mixture, which was before to the introduction of the gas stream. Before this test, pure water had been tested in the pilot as well. Thus, this sample should be representative of the initial absorption mixture with potentially a small amount of additional water. Table 13 shows that the analysis of the L1 sample gives an AMP concentration of 20.76 wt% and a DMSO concentration of 64.28 wt% (which is a ratio of about 1 to 3, AMP to DMSO). This is a reasonable result since the absorption mixture was prepared with an AMP to DMSO volume ratio of roughly 1 to 3. The remaining part of the sample is likely water, which cannot be detected with an FID-detector.

The samples L2, L3 and L4 were all collected after the absorption mixture had been connected to the gas stream in the pilot. These samples contained some precipitate and only the liquid phase was analyzed. Table 13 shows an AMP concentration of approximately 11 wt% for all these samples and a DMSO concentration of around 42 wt% for sample L2 and around 55 wt% for sample L3 and L4. The variation in DMSO concentrations likely arise from the diverse operating parameters applied when the samples were taken. Samples L3 and L4 were taken on

different occasions while the stripper tank was being emptied. L3 was taken at the start and L4 when half of the tank had been emptied. This makes sample L3 representable of the bottom part of the tank and L4 of the middle part of the tank. The fact that the analysis resulted in comparable concentrations for these samples implies that there was no significant difference in composition between the different regions in the stripper tank, suggesting a homogeneous mixture. It should however be noted that the reason to why L3 and L4 are within each outer's uncertainty range could be because of the large standard deviations for these samples, which becomes evident from the standard uncertainty percentages. If more precise results were required, these samples might need to be reanalyzed.

That L2, L3, and L4 have lower concentrations compared to L1, for both AMP and DMSO, is expected since the gas stream introduces several different compounds into the pilot. However, it seems like the amount of AMP decreases to a higher degree than the amount of DMSO (with an AMP to DMSO ratio of about 1 to 4 for L2 and 1 to 5 for L3 and L4). This suggests that AMP has participated in a chemical reaction of some kind. One likely scenario is that AMP reacts with CO_2 from the gas stream to form the carbamate, as described in Section 2.2, and this could potentially be the observed precipitate in these samples. However, further investigations would be required to determine if the carbamate or some other reaction product has been formed.

Sample S1 and S2 were taken from the precipitation on the inside and outside of the lean solvent pipe (S1 on the inside and S2 on the outside). The analysis shows that the two solid samples have higher concentrations of AMP than DMSO than the liquid samples, with 49.82 wt% AMP and 19.91 wt% DMSO for S1 and 57.00 wt% AMP and 19.93 wt% DMSO for S2. This could be explained with the reaction of AMP and CO_2 with resulting carbamate formation, since a large amount of carbamate would be expected to be present in the precipitate. But, as mentioned, further investigations would be required to confirm that the solid precipitate formed in the pilot plant is the AMP carbamate.

The analysis of the AMP feedstock, sample L6, suggested an AMP concentration of about 100.0 wt%. The concentration was expected to be between 90 – 100 vol%, with up to 10 vol% impurities, and the result is hence not unreasonable. The value of the standard deviation did however turn out relatively high, with 5.521. This makes the result less legitimate, but it could suggest that the concentration is within the higher regions of the expected concentration range.

The condensed liquid sample (sample L5) gave no detector response for AMP or DMSO when diluted with the dilution factor 20.8 (sample L5a) and 10 (sample L5b). Some response for DMSO was however obtained when the sample was diluted with a dilution factor of 5 (sample L5c), which resulted in a concentration of 0.4493 wt%, as listed in Table 13. It should be noted that since these samples were taken from gas that had condensed and been collected at the sampling spot, these samples cannot be assumed to fully represent the gas stream and the result should only be interpreted as an indication of the composition.

None of the gas samples generated any detector response for AMP. Samples G1_1 and G1_2 generated a small DMSO response, resulting in the concentrations 0.3233 wt% and 0.07147 wt% respectively. This indicates that DMSO potentially can end up in the gas-outlet-stream from the pilot. These results do however only give the concentrations in the extracted samples from the certified lab and does not provide much information about the concentration in the gas

stream at the pilot. These concentrations were therefore used to calculate the amount of DMSO in the samples, which could then be used to give an estimation of the DMSO concentration in the pilot plant gas stream. These calculations are given in Appendix E and results in the concentration in Table 14 below.

Table 14. Shows the DMSO concentration in the gas outlet stream from the pilot. The calculations providing this result are given in Appendix E. Since G1_1 and G1_2 arise from the same sample, they are here combined into one, sample G1, to give the total DMSO concentration.

	DMSO concentration in pilot plant gas outlet stream
G1	40 mg/m^3

It should be noted that this concentration was derived during a period when the gas cleaning process was not in operation. It should also be noted that this is the concentration in the gas outlet stream from the pilot plant. This stream is mixed with the gas stream from the chimney on the industrial site, where it was initially taken, before it is released into the atmosphere. This dilution will make the emitted DMSO concentration to be considerably lower than the one calculated in Table 14. The result from this analysis hence suggests that only small concentrations of AMP and DMSO are emitted from the pilot plant.

5 Conclusion

The experimental findings presented in this study demonstrate that GC can be used successfully for both qualitative and quantitative analysis of AMP and DMSO. The qualitative analysis section of the thesis shows that acetonitrile outperforms the other solvents. Acetonitrile can provide chromatograms with constant retention times and sufficient separation, with resolutions above 1.5. This indicates that AMP and DMSO can be identified in a mixture containing both, when solved in acetonitrile. The poor and inconsistent results observed for sulfamic acid and sulfuric acid as solvents may be attributed to their dilution with water. Water has a large expansion volume and can occasionally extinguish the detector flame, resulting in varying retention times and peak sizes. The use of non-polar columns for the polar water solvents could also have contributed to the fluctuating results and further investigations would have to be conducted to investigate the full potential of these solvents. These findings emphasize the importance of using appropriate equipment and solvents when performing GC analyses.

The quantitative analysis section of this thesis shows potential for using both the external standard method and the internal standard method for quantifying AMP and DMSO. In both methods, linear relationships between concentration and detector response can be obtained, with R_2-values exceeding 0.99 and a random scatter of residuals for all calibration curves. The comparison of linear regressions for the external calibration curves with AMP as the single analyte and AMP mixed with DMSO suggests that the presence of DMSO might affect the AMP response. This could be attributed to variations in GC parameters across different tests or that the response has different linearity over the different concentration ranges. These results imply that calibration curves should be produced in close temporal proximity to the analysis of the sample, and with a relatively narrow concentration range around the anticipated concentration.

The outlier test in the qualitative section of this thesis suggests that outliers do not affect the results of the linear regressions significantly. For the external calibration curves, outliers seem to be averaged out effectively, while for the internal calibration curves, all peaks seem to be affected to a similar extent, which does not influence the ratios. Additionally, the use of MEA as an internal standard proves to be effective, with constant retention times and sufficient separation from the analytes. Since the internal standard was only tested on lab-prepared samples, further tests would have to be performed on actual samples from the pilot plant, with additional unknown components present, to investigate the full potential of the method.

The analysis of the samples from the pilot plant yields reasonable results for the initial absorption mixture, with a 1 to 3 weight ratio of AMP to DMSO. This validates the analysis method and suggests that the external standard method, with the developed GC method settings and acetonitrile as the solvent, can give an approximate estimation of the composition of AMP and DMSO for a sample from the pilot plant.

The comparison in composition between the initial absorption mixture and the mixture after the introduction of the gas stream, indicates that AMP participates in a reaction in the pilot, as expected. This since the wt% of AMP decreases more than the wt% of DMSO for all analyzed samples after the gas stream introduction. This is likely due to carbamate formation, when AMP reacts with CO_2 in the flue gas, which is expected to be formed in the system. However, further investigations are required to identify the reaction products.

The analysis of the samples taken at the gas-streams from the pilot plant results in low AMP and DMSO concentrations. No AMP could be detected with the used method and only small amounts of DMSO. The estimated DMSO concentration in the gas-outlet-stream from the pilot plant proved to be low, especially considering that this gas-stream is diluted with the gas-stream from the industrial site before it is released into the atmosphere. The result in this thesis therefore suggests that only small concentrations of AMP and DMSO are emitted from the pilot plant.

6 Future work

Samples from the pilot had to be taken regularly and analyzed throughout its operating time at VEAB. Therefore, in this thesis, they were exclusively analyzed with the external standard method, since it was the method first developed and evaluated. The internal standard method was only tested on lab-prepared samples. Since the internal standard method showed such promising results, it would be of interest to carry out further testing to investigate its potential for analyzing more complex samples from the pilot. A comparison between concentrations for the same sample, obtained from the two methods, could also give further insights into their legitimacy of representing reality.

In this thesis, the methods were validated based on linearity, selectivity and precision. This gives a solid foundation when examining the suitability of the methods for their intended purposes. However, additional validation parameters could be implemented to further evaluate the methods. One example is accuracy, which can be interpreted as how close the analysis represents the truth. This can be done by comparing the results with the ones from other analytical methods. In this thesis, GC was the only analytical method used and further investigations into other possible methods could be of interest to evaluate the accuracy of the results. Another way of measuring accuracy, which is the commonly practiced in GC applications, is by using standard additions. The implementation of standard additions could be of interest for future research. Another validation parameter that might be of interest for future studies, which was not investigated in this thesis, is range. The range refers to the concentration interval over which the method can be used for valid analyses and could provide an insight into which kind of samples can be analyzed with the methods.

Investigations into what causes the tendency to tilt with a slight negative slope in the lower concentration for the external calibration curves for AMP could be of interest. Additional analyses would have to be carried out to determine whether it is caused by a shift in linearity between the concentration ranges, or if it is caused by random errors.

A carbamate formation is expected to occur in the pilot plant environment when AMP reacts with CO_2 in the flue gas. The result from this thesis indicates that this is the case, however, further investigations would be required to identify the reaction products.

7 References

(1) Climate Change 2022 - Mittigation of Climate Change. Intergovernmental Panel on Climate Change: 2022.
(2) KYOTO PROTOCOL TO THE UNITED NATIONS FRAMEWORK CONVENTION ON CLIMATE CHANGE. United Nations: Kyoto, 1997; Vol. Third session.
(3) PARIS AGREEMENT. United Nations: Paris, 2015.
(4) Shaftel, H.; Callery, S.; Jackson, R.; Bailey, D. *Vital Signs - Carbon Dioxide*. NASA Global Climate Change, https://climate.nasa.gov/vital-signs/carbon-dioxide/ (accessed 2023-06-06).
(5) Sabine, C. L.; Feely, R. A. CARBON DIOXIDE. *Encyclopedia of Atmospheric Sciences* **2002**, 335-343.
(6) Industrin – nuläge och förutsättningar för omställning. Statens energimyndighet: 2021.
(7) Bandilla, K. W. Carbon Capture and Storage. In *Future Energy*, 2020; pp 669-692.
(8) Moriarty, P.; Honnery, D. Bioenergy with carbon capture and storage in a future world. In *Bioenergy with Carbon Capture and Storage*, 2019; pp 273-287.
(9) Karlsson, H. Precipitating Amine Absorption Systems for Carbon Capture. Doctoral Dissertation, Department of Chemical Engineering, Lund University, 2021.
(10) Li, K.; White, S.; Zhao, B.; Geng, C.; Halliburton, B.; Wang, Z.; Zhao, Y.; Yu, H.; Yang, W.; Bai, Z.; et al. Evaluation of a New Chemical Mechanism for 2-Amino-2-methyl-1-propanol in a Reactive Environment from CSIRO Smog Chamber Experiments. *Environ Sci Technol* **2020**, *54* (16), 9844-9853. DOI: 10.1021/acs.est.9b07669 From NLM Medline.
(11) Fostås, B.; Gangstad, A.; Nenseter, B.; Pedersen, S.; Sjøvoll, M.; Sørensen, A. L. Effects of NOx in the flue gas degradation of MEA. *Energy Procedia* **2011**, *4*, 1566-1573. DOI: 10.1016/j.egypro.2011.02.026.
(12) Finney, K. N.; Akram, M.; Diego, M. E.; Yang, X.; Pourkashanian, M. Carbon capture technologies. In *Bioenergy with Carbon Capture and Storage*, 2019; pp 15-45.
(13) Dubey, A.; Arora, A. Advancements in carbon capture technologies: A review. *Journal of Cleaner Production* **2022**, *373*. DOI: 10.1016/j.jclepro.2022.133932.
(14) Cuccia, L.; Dugay, J.; Bontemps, D.; Louis-Louisy, M.; Vial, J. Analytical methods for the monitoring of post-combustion CO2 capture process using amine solvents: A review. *International Journal of Greenhouse Gas Control* **2018**, *72*, 138-151. DOI: 10.1016/j.ijggc.2018.03.014.
(15) <proceduresformanualsampling_csiro-2.pdf>.
(16) Harris, D. C.; Lucy, C. A. *QUANTITATIVE CHEMICAL ANALYSIS*; Macmillan Learning, 2020.
(17) Chapter 1 Introduction and Definitions. In *For Laboratory Analyses and On-Line Process Control*, Journal of Chromatography Library, 1988; pp 1-34.
(18) Poole, C. F. Column technology. In *Gas Chromatography*, 2021; pp 141-163.
(19) Dorman, F. L.; Dawes, P. Column technology. In *Gas Chromatography*, 2021; pp 99-116.
(20) Ojanperä, I.; Rasanen, I. Chapter 11 Forensic screening by gas chromatography. In *Forensic Science*, Handbook of Analytical Separations, 2008; pp 403-424.
(21) *Application Note: Carrier gases and their differences*. Scion Instruments, https://scioninstruments.com/application-note-carrier-gases-and-their-differences/ (accessed 2023-06-06).
(22) Han, Y.; Zhang, Y.; Liu, H. Gas Chromatography: Principles ☆. In *Reference Module in Chemistry, Molecular Sciences and Chemical Engineering*, 2017.
(23) Lewis, P. R. Small Containers. In *Forensic Polymer Engineering*, 2016; pp 147-190.

(24) Fujimoto, T.; Takeda, K.; Nonaka, T. Airborne Molecular Contamination. In *Developments in Surface Contamination and Cleaning*, 2008; pp 197-329.
(25) Snow, N. H. Temperature Programed GC: Why Are All Those Peaks So Sharp? *LCGC North America* **2019**, *37* (7), 450-456.
(26) *GC Troubleshooting Guide*. Agilent Technologies, 2023. https://www.agilent.com/cs/library/posters/public/5994-0451EN_GC_Troubleshooting_Guide%20poster_LR.pdf (accessed 2023-02-01).
(27) Kivijärvi, H.; Kollberg, L.; Sundin, M. Determining CO2 loading. Advanced course project, Lund University, Lund, 2019.
(28) Meng, F.; Fu, K.; Wang, X.; Wang, Y.; Wang, L.; Fu, D. Study on absorption and regeneration performance of EHA-DMSO non-aqueous absorbent for CO2 capture from flue gas. *Energy* **2024**, *286*. DOI: 10.1016/j.energy.2023.129631.
(29) English, C. Injecting Water onto a GC Column: Solving the Mystery of Poor Chromatography. *The Column* **2018**, *14* (6), 18-22.

Appendix A – GC Method Settings for Acetonitrile and Sulfuric acid

This appendix presents two GC method settings that gave the best results for the tests involving acetonitrile and sulfuric acid as the solvent. Consequently, these settings were employed for all analyses when acetonitrile and sulfuric acid as the solvent. The settings were found by trial and error and were initially based on the settings used in a project performed at Lund University, where a method was created for GC analysis of AMP and NMP (n-methyl-2-pyrrolidon) with ethanol as solvent[27]. The difference between the two method settings is the split ratio, which is 50:1 for the first one and 5:1 for the second one. Consequently, the total flow in the inlet is adjusted. The settings are listed in Table A.1 and Table A.2.

Table A.1. Lists the GC method settings with 50:1 as the split ratio. It was used for most analyses when acetonitrile or sulfuric acid were used as the solvent.

Acquisition Method – DW_Method_AMP_DMSO.amx

ALS

> Front Injector

Injection

Injection volume:	1 µL

Washes and Pumps

	PreInj	PostInj	Volume (µL)
SolventA Washes	0	5	Max(8)
SolventB Washes	0	5	Max(8)
Sample Washes	0		Max(8)
Sample Pumps	3		

Dwell Time

Pre-Injection	0 min
Post-Injection	0 min

Plunger Depth:	Slow
Injection type:	Standard
L1 air gap:	0.2 µL

> Inlets

Heater:	255 C
Pressure:	0.59204 bar
Total flow:	79.5 mL/min
Septum Purge Flow:	3 mL/min

Inlet Mode: Split

Split ratio: 50:1 Split Flow: 75 mL/min

Gas Saver: Off

> Columns

Control Mode: On

Flow

Pressure:	0.59204 bar
Average Velocity:	29.697 cm/sec
Holdup Time:	1.6837 min

Carrier gas: N_2

> Oven

	Rate [°C/min]	Value [°C]	Hold Time [min]	Run Time [min]
(Initial)		100	1	1
Ramp 1	30	240	0	5.6667

Detector

> Front Detector FID

Heater:	255 °C
Air Flow:	400 mL/min
H_2 Fuel Flow:	30 mL/min
Makeup Flow (N_2)	10 mL/min

Table A.2. Lists the GC method settings with split ratio 5:1. It was used for the analysis of the gaseous pilot plant samples, with acetonitrile as the solvent.

Acquisition Method – DW_Method_AMP_DMSO_Acetonitrile_split5.amx

ALS

> Front Injector

Injection

Injection volume:	1 µL

Washes and Pumps

	PreInj	PostInj	Volume (µL)
SolventA Washes	0	5	Max(8)
SolventB Washes	0	5	Max(8)
Sample Washes	0		Max(8)
Sample Pumps	3		

Dwell Time

Pre-Injection	0 min
Post-Injection	0 min

Plunger Depth: Slow

Injection type: Standard

L1 air gap:	0.2 µL

> Inlets

Heater:	255 C			
Pressure:	0.59204 bar			
Total flow:	12 mL/min			
Septum Purge Flow:	3 mL/min			
Inlet Mode:	Split			
	Split ratio:	5:1	Split Flow:	75 mL/min
Gas Saver:	Off			

> Columns

Control Mode: On

Flow

Pressure:	0.59204 bar
Average Velocity:	29.697 cm/sec
Holdup Time:	1.6837 min

Carrier gas: N_2

> Oven

	Rate [°C/min]	Value [°C]	Hold Time [min]	Run Time [min]
(Initial)		100	1	1
Ramp 1	30	240	0	5.6667

Detector

> Front Detector FID

Heater:	255 °C
Air Flow:	400 mL/min
H_2 Fuel Flow:	30 mL/min
Makeup Flow (N_2)	10 mL/min

Appendix B – GC Method Settings for Sulfamic acid

This appendix presents the GC method settings that gave the best results for the tests involving aqueous sulfamic acid as the solvent. These settings were therefore used for the analyses where sulfamic acid was used as the solvent. The settings are listed in Table A.2.

Table B.1. Lists the GC method settings used for all analyses when sulfamic acid was used as the solvent.

Acquisition Method – DW_Method_AMP_DMSO_SulfamicAcid_90to240_ramp7.5_hold1min175.amx

ALS

> Front Injector

Injection

Injection volume:	1 µL

Washes and Pumps

	PreInj	PostInj	Volume (µL)
SolventA Washes	0	5	Max(8)
SolventB Washes	0	5	Max(8)
Sample Washes	0		Max(8)
Sample Pumps	3		

Dwell Time

Pre-Injection	0 min
Post-Injection	0 min

Plunger Depth:	Slow
Injection type:	Standard
L1 air gap:	0.2 µL

> Inlets

Heater:	255 C
Pressure:	0.57007 bar
Total flow:	79.5 mL/min
Septum Purge Flow:	3 mL/min
Inlet Mode:	Split

	Split ratio:	50:1	Split Flow:	75 mL/min

Gas Saver: Off

> Columns

Control Mode: On

Flow

Pressure:	0.57007 bar
Average Velocity:	29.173 cm/sec
Holdup Time:	1.7139 min

Carrier gas: N_2

> Oven

	Rate [°C/min]	Value [°C]	Hold Time [min]	Run Time [min]
(Initial)		90	1	1
Ramp 1	7.5	175	1	13.333
Ramp 2	7.5	240	0	22

Detector

> Front Detector FID

Heater:	255 °C
Air Flow:	400 mL/min
H_2 Fuel Flow:	30 mL/min
Makeup Flow (N_2)	10 mL/min

Appendix C – External calibration curves for pilot plant sample set 1

This appendix presents the values, results and calculations for the analysis of the first set of samples from the pilot plant. A five-point calibration curve was created for each analyte (AMP and DMSO). First, the calibration standard samples were prepared in the lab, resulting in the concentrations listed in Table C.1.

Table C.1. Shows the concentrations of AMP and DMSO in the dilution series used for the calibration curves for the first set of pilot plant samples.

	wt% AMP	wt% DMSO
1AAD	1.654	4.631
2AAD	1.332	3.729
3AAD	0.9031	2.529
4AAD	0.3473	0.9724
5AAD	0.1278	0.3577

These standards were then analyzed three times each in the GC with the method settings presented in Table A.1, in Appendix A. The resulting GC areas are presented in Table C.2.

Table C.2. Lists the areas obtained from the GC analysis of the calibration standards. Each standard was analyzed three times, indicated by number 1, 2 and 3 under AMP and DMSO. The average area for each standard is also listed. This table displays the values with four significant figures.

	AMP				DMSO			
	1	**2**	**3**	**Average**	**1**	**2**	**3**	**Average**
1AAD	2352	2654	2683	2563	6643	6860	6744	6746
2AAD	3044	2098	2144	2095	5740	5518	5564	5607
3AAD	1306	1364	1378	1349	3832	3694	3600	3708
4AAD	413.1	489.2	512.4	471.5	1381	1471	1422	1425
5AAD	102.1	132.1	132.1	122.1	467.4	472.5	423.4	454.4

The average area for each standard were then plotted against their respective concentrations in Table C.1, resulting in the external calibration curves in Figure C.1.

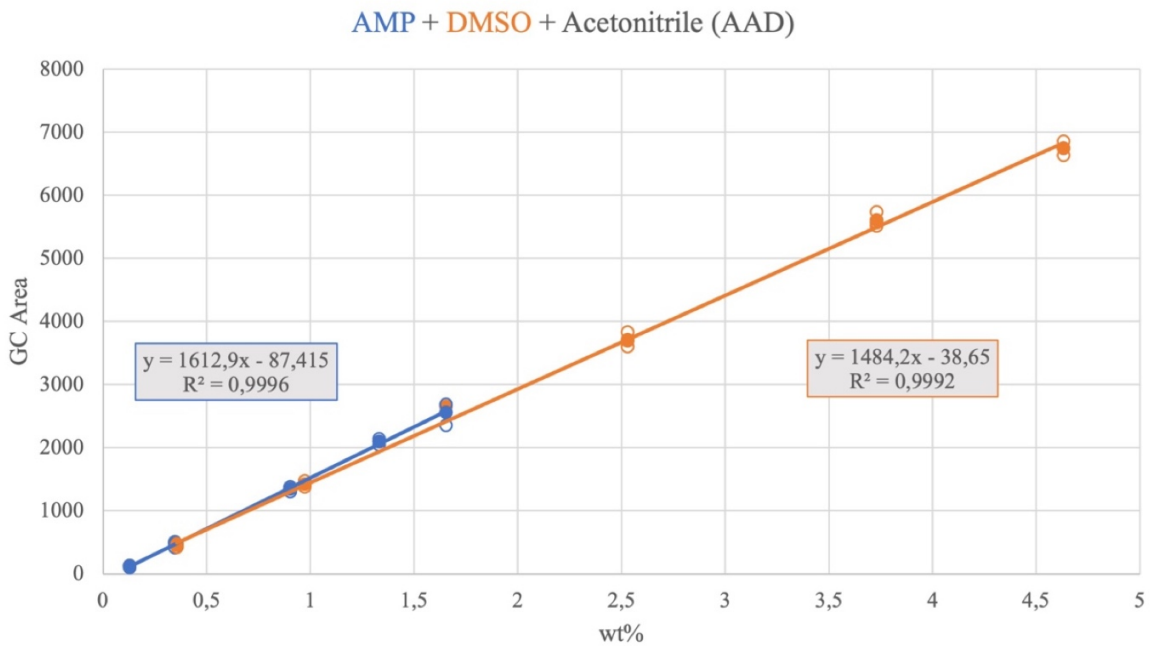

Figure C.1. Shows the calibration curves used for the analysis of the first set of samples from the pilot plant. Blue represents AMP and orange represents DMSO. The measured areas are indicated with unfilled circles and the average of these, from which the linear regressions are based on, are indicated with filled circles.

The linear regressions of each curve are summarized in Table C.3.

Table C.3. Summarizes the k- and m-vales of the linear regressions in Figure C.1.

	k	**m**
AMP	1612.9	-87.415
DMSO	1484	-38.65

Four samples were analyzed with these linear regressions, sample L1, L2, S1 and S2. The results of the GC analysis of these samples are presented in Table C.4.

Table C.4. Lists the areas obtained from the GC analysis of the first set of samples. The liquid sample was analyzed three times and the solid samples two times, indicated by number 1, 2 and 3 under AMP and DMSO. The average area for each sample is also listed. This table displays the values with four significant figures.

	AMP				**DMSO**			
	1	**2**	**3**	**Average**	**1**	**2**	**3**	**Average**
L1	1324	1374	1511	1403	4139	4145	4346	4210
L2	677.1	691.9	709.5	692.8	2701	2667	2698	2688
S1	194.0	198.2	-	196.1	64.83	59.91	-	62.37
S2	201.8	206.2	-	204.0	54.40	48.67	-	51.53

It should be noted that the DMSO areas for the solid samples received areas outside of the concentration range covered by the calibration curve. The following calculations hence approximate the same linearity as the calibration curve as for the concentration range in which the sample ended up. For an ideal analysis, the samples could have been diluted less, or a new calibration curve that would cover the concentration range could have been constructed.

The average areas were then used as the y-value in Equation C.1.

$$x = \frac{(y - m)}{k} DF \tag{C.1}$$

The k- and m-values are the once in Table C.3. The dilution factors (DF) for each sample are listed in Table C.5, together with the calculated concentrations.

Table C.5. Lists the calculated concentrations for the first set of samples from the pilot plant. The dilution factors (DF), standard deviations (STD) and percentage standard deviations (STD%) are also given.

	DF	**wt% AMP**	**STD**	**STD%**	**wt% DMSO**	**STD**	**STD%**
L1	22.00	20.76	1.105	5.322	64.28	1.454	2.262
L2	22.82	11.04	0.1874	1.698	41.93	0.2367	0.5646
S1	286.0	50.20	0.3731	0.7434	19.44	0.4730	2.433
S2	318.0	57.43	0.4291	0.7472	19.31	0.6127	3.172

These results are also given in Table 13, Section 4.3.

Appendix D – External calibration curves for pilot plant sample set 2

This appendix presents the values, results and calculations for the analysis of the second set of samples from the pilot plant. A ten-point calibration curve was created for each analyte (AMP and DMSO). First, the calibration standard samples were prepared in the lab, resulting in the concentrations listed in Table D.1.

Table D.1. Shows the concentrations of AMP and DMSO in the dilution series used for the calibration curves for the first set of pilot plant samples.

	wt% AMP	wt% DMSO
1AAD	4.945	5.095
2AAD	4.330	4.461
3AAD	3.341	3.442
4AAD	2.419	2.492
5AAD	1.538	1.585
6AAD	1.092	1.126
7AAD	0.8070	0.8315
8AAD	0.5259	0.5418
9AAD	0.2730	0.2813
10AAD	0.09995	0.1023

These standards were then analyzed three times each in the GC with the method settings presented in Table A.1, in Appendix A. The resulting GC areas are presented in Table D.2.

Table D.2. Lists the areas obtained from the GC analysis of the calibration standards. Each standard was analyzed three times, indicated by number 1, 2 and 3 under AMP and DMSO. The average area for each standard is also listed. This table displays the values with four significant figures.

	AMP				DMSO			
	1	**2**	**3**	**Average**	**1**	**2**	**3**	**Average**
1AAD	7678	9092	8913	8561	6556	6699	6245	6500
2AAD	7040	8054	7924	7673	5860	5835	5612	5769
3AAD	4209	6167	6125	5500	3121	4551	4341	4017
4AAD	4106	4437	4594	4379	3460	3437	3321	3406
5AAD	1811	2742	2630	2394	1436	2227	2088	1917

6AAD	1272	1973	2060	1768	996.5	1600	1581.6	1393
7AAD	1213	1492	1544	1416	1115	1212	1208	1178
8AAD	742.3	918.8	939.9	867.0	688.3	745.6	756.3	730.1
9AAD	447.7	462.2	463.6	457.9	419.7	385.2	394.0	399.6
10AAD	91.70	131.7	170.6	131.3	90.56	132.4	147.8	123.6

The average area for each standard were then plotted against their respective concentrations in Table D.1, resulting in the external calibration curves in Figure D.1.

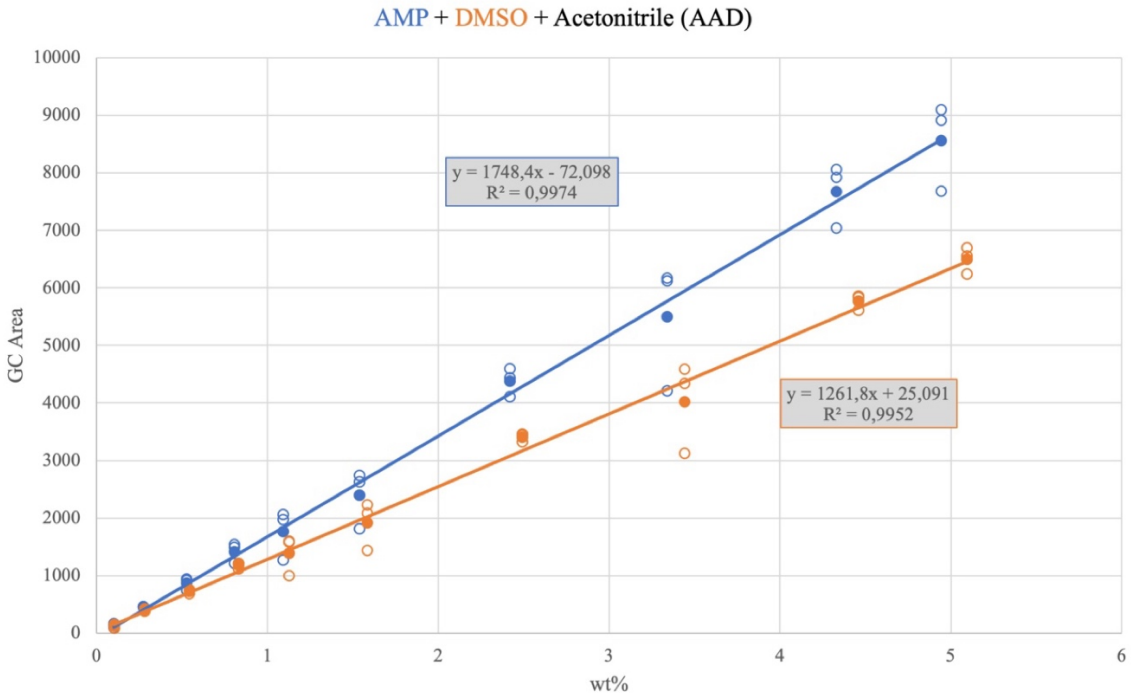

Figure D.1. Shows the calibration curves used for the analysis of the second set of samples from the pilot plant. Blue represents AMP and orange represents DMSO. The measured areas are indicated with unfilled circles and the average of these, from which the linear regressions are based on, are indicated with filled circles.

The linear regressions of each curve are summarized in Table D.3.

Table D.3. Summarizes the k- and m-vales of the linear regressions in Figure D.1.

	k	**m**
AMP	1748.4	-72.098
DMSO	1261.8	25.091

Six samples were analyzed with these linear regressions, sample L3, L4, L5a, L5b, L5c and L6. The results of the GC analysis of these samples are presented in Table D.4.

Table D.4. Lists the areas obtained from the GC analysis of the second set of samples. The sample was analyzed three times, indicated by number 1, 2 and 3 under AMP and DMSO. The average area for each sample is also listed. This table displays the values with four significant figures.

	AMP				DMSO			
	1	**2**	**3**	**Average**	**1**	**2**	**3**	**Average**
L3	813.4	757.5	966.9	845.9	3370	3149	3400	3306
L4	659.5	942.5	986.5	862.8	3042	3503	3464	3336
L5a	-	-	-	-	52.75	50.43	50.91	51.36
L5b	-	-	-	-	-	95.13	120.7	71.93
L5c	-	-	-	-	196.6	202.0	198.3	199.0
L6	7664	8629	8664	8319	-	-	-	-

The average areas were then used as the y-value in Equation C.1. The k- and m-values were taken from Table D.3. The dilution factors (DF) for each sample are listed in Table D.5, together with the calculated concentrations.

Table D.5. Lists the calculated concentrations for the second set of samples from the pilot plant. The dilution factors (DF), standard deviations (STD) and percentage standard deviations (STD%) are also given.

	DF	**wt% AMP**	**STD**	**STD%**	**wt% DMSO**	**STD**	**STD%**
L3	20.8	10.93	1.054	9.641	54.15	1.847	3.411
L4	21.0	11.23	1.741	15.50	55.15	3.476	6.308
L5a	20.8	-	-	-	-	-	-
L5b	10.0	-	-	-	-	-	-
L5c	5.00	-	-	-	0.4493	0.008971	1.997
L6	20.8	100.0	5.521	5.519	-	-	-

These results are also given in Table 13, Section 4.3.

Appendix E – External calibration curves for pilot plant sample set 3

This appendix presents the values, results and calculations for the analysis of the third set of samples from the pilot plant, the gaseous samples. A ten-point calibration curve was created for DMSO (these samples did not receive any AMP response and hence no AMP-calibration curve was created, see Table E.4). First, the calibration standard samples were prepared in the lab, resulting in the concentrations listed in Table E.1.

Table E.1. Shows the concentrations of DMSO in the dilution series used for the calibration curve for the third set of pilot plant samples. It should be noted that the standards did contain AMP as well, but since the gaseous pilot samples did not give any response for AMP, an AMP-calibration curve was not constructed, and the AMP concentrations is therefore not displayed.

	wt% DMSO
1AAD	0.5322
2AAD	0.4253
3AAD	0.3777
4AAD	0.2499
5AAD	0.1425
6AAD	0.1154
7AAD	0.08869
8AAD	0.07125
9AAD	0.03264
10AAD	0.01002

These standards were then analyzed three times each in the GC with the method settings presented in Table A.2i in Appendix A. The resulting GC areas are presented in Table E.2.

Table E.2. Lists the areas obtained from the GC analysis of the calibration standards. Each standard was analyzed three times, indicated by number 1, 2 and 3 DMSO. The average area for each standard is also listed. This table displays the values with four significant figures.

	DMSO			
	1	**2**	**3**	**Average**
1AAD	1540	2088	2117	1915
2AAD	1550	1254	1188	1331
3AAD	1475	1058	1375	1303

4AAD	908.8	841.1	715	821.9
5AAD	469.1	488.6	405.0	454.2
6AAD	348.0	349.7	333.3	343.7
7AAD	273.5	270.8	298.1	280.8
8AAD	225.4	221.8	212.5	219.9
9AAD	130.9	103.3	106.2	104.5
10AAD	31.81	32.07	31.54	31.81

The average area for each standard were then plotted against their respective concentrations in Table E.1, resulting in the external calibration curves in Figure E.1.

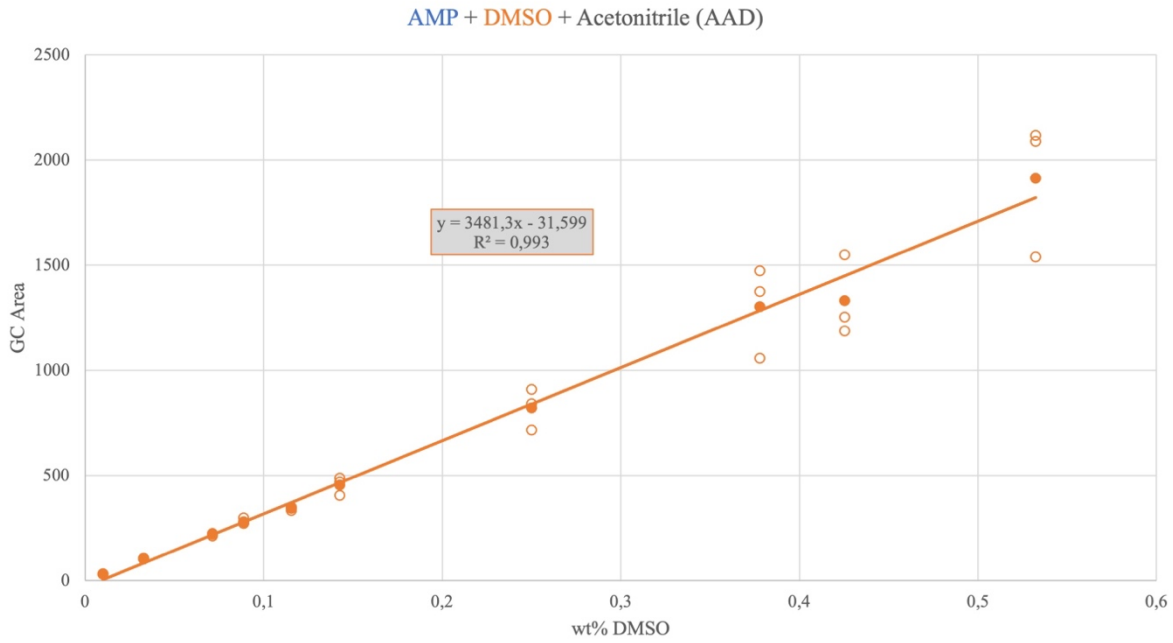

Figure E.1. Shows the calibration curves used for the analysis of the gaseous samples from the pilot plant. The measured areas are indicated with unfilled circles and the average of these, from which the linear regression is based on, are indicated with filled circles.

The linear regressions of each curve are summarized in Table E.3.

Table E.3. Summarizes the k- and m-vales of the linear regression in Figure E.1.

	k	**M**
DMSO	3481.3	-31.599

The two gas samples, G1 and G2, were analyzed using this linear regression. These samples were taken using the cartridge method, where the thermosorbs first were sent to a certified lab before the samples were analyzed for this thesis at the department at Lund University. The

certified lab first added 50 µL internal standard (25 µg/ml NDMA) to the thermosorbs and then extracted with 2 ml acetonitrile. One of the samples was extracted one time, noted sample G2 in this thesis. The other sample, G1 was extracted two times, resulting in two samples, G1_1 and G1_2. The amount of analyte found in G1_1 and G1_2 would hence need to be added together to represent the amount of sample G1.

The results of the GC analysis of these samples are presented in Table E.4.

Table E.4. Lists the areas obtained from the GC analysis of the gaseous samples. The sample was analyzed three times, indicated by number 1, 2 and 3 under AMP and DMSO. The average area for each sample is also listed. This table displays the values with four significant figures.

	AMP				DMSO			
	1	**2**	**3**	**Average**	**1**	**2**	**3**	**Average**
G1_1	-	-	-	-	1195	1086	1002	1094
G1_2	-	-	-	-	229.1	218.6	204.0	217.2
G2	-	-	-	-	81.59	55.13	42.551	59.76

The average areas were used as the y-value in Equation C.1. The k- and m-values were taken from Table E.3 to calculate the concentrations in Table E.5. Even though there was a small DMSO response given for G2, it was too low to give any valid concentration estimation.

Table E.5. Lists the calculated concentrations for the second set of samples from the pilot plant. The standard deviations (STD) and percentage standard deviations (STD%) are also given.

	wt% AMP	**STD**	**STD%**	**wt% DMSO**	**STD**	**STD%**
G1_1	-	-	-	0.3233	0.02273	0.07031
G1_2	-	-	-	0.07147	0.002957	0.04138
G2	-	-	-	-	-	-

The results in Table E.5 does however only give the concentration in the extracted samples and does not provide too much information about the concentration in the gas stream at the pilot. These concentrations were therefore used to calculate the amount of DMSO, which could then be used to give an estimation of the DMSO concentration in the pilot plant gas stream. These calculations are given below.

To calculate the mass of DMSO in the sample, assumptions needed to be made. It was assumed that the samples had the same density as pure acetonitrile, 0.786 g/mL, (since the DMSO and NDMA concentrations are so small) and that the volumes of the samples were the volume of acetonitrile used for the extractions, 2 mL. The mass could then be calculated using Equation E.1.

$$m_{DMSO,sample} = \frac{c_{DMSO,sample}}{100} V_{acetonitrile} \rho_{acetonitrile} \quad \text{(E.1)}$$

Where m_{DMSO} is the mass of DMSO, c_{DMSO} is the concentration of DMSO in wt%, $V_{acetonitrile}$ is the volume of acetonitrile and $\rho_{acetonitrile}$ is the density of acetonitrile. The mass of DMSO in sample G1_1 and G1_2 was then added together to give the mass in sample G1.

Table E.6. The mass of DMSO in mg for the samples making up G1. The results are given with four significat figures.

G1_1 [mg]	G1_2 [mg]	G1 [mg]
5.083	1.123	6.206

The DMSO concentration in the pilot plant can then be calculated with the volume of gas used to collect the sample, according to Equation E.2.

$$c_{DMSO,pilot\ plant} = \frac{m_{DMSO,samples}}{V_{gas}} \quad \text{(E.2)}$$

Using Equation E.2, with the mass for G1 and the gas volume of 156.67 L (measured in the thesis work *Operating procedures and evaluation of a carbon capture pilot plant* by Isac Logeke at the Department of Chemical Engineering) results in the concentration listed in Table E.7.

Table E.7. Shows the DMSO concentration in the gas outlet stream from the pilot, calculated from the measured results in Table E.5.

	DMSO concentration in pilot plant gas outlet stream
G1	40 mg/m^3

These results are also given in Section 4.3. It should be noted that this concentration was derived during a period when the gas cleaning process was not in operation. It should also be noted that this is the concentration in the gas outlet stream from the pilot plant. This stream is mixed with the gas stream from the chimney on the industrial site, where it was initially taken, before it is released into the atmosphere. This dilution will make the emitted DMSO concentration to be considerably lower than the one calculated here.